JHEP04(2016)144

The renormalized Hamiltonian truncation method in the large E_T expansion

J. Elias-Miró,[a] M. Montull[b] and M. Riembau[b,c]

[a]*SISSA and INFN,*
I-34136 Trieste, Italy

[b]*Institut de Física d'Altes Energies (IFAE), Barcelona Institute of Science and Technology (BIST),*
Campus UAB, E-08193 Bellaterra, Spain

[c]*DESY,*
Notkestrasse 85, 22607 Hamburg, Germany

E-mail: jelias@sissa.it, mmontull@ifae.es, marc.riembau@desy.de

ABSTRACT: Hamiltonian Truncation Methods are a useful numerical tool to study strongly coupled QFTs. In this work we present a new method to compute the exact corrections, at any order, in the Hamiltonian Truncation approach presented by Rychkov et al. in refs. [1–3]. The method is general but as an example we calculate the exact g^2 and some of the g^3 contributions for the ϕ^4 theory in two dimensions. The coefficients of the local expansion calculated in ref. [1] are shown to be given by phase space integrals. In addition we find new approximations to speed up the numerical calculations and implement them to compute the lowest energy levels at strong coupling. A simple diagrammatic representation of the corrections and various tests are also introduced.

Contents

1 Introduction and review

An outstanding problem in theoretical physics is to solve strongly coupled Quantum Field Theories (QFT). When they are not amenable to analytic calculations one can resort to numerical approaches. The two most used numerical approaches are lattice simulations and direct diagonalization of truncated Hamiltonians. In this paper we further develop the Hamiltonian truncation method recently presented in ref. [1–3], that renormalizes the truncated Hamiltonian H_T to improve the numerical accuracy.

The Hamiltonian truncation method consists in truncating the Hamiltonian H into a large finite matrix $(H_T)_{ij}$ and then diagonalizing it numerically. There is a systematic error with this approach that vanishes as the size of the truncated Hamiltonian H_T is increased. There are different versions of the Hamiltonian truncation method that mainly differ on the frame of quantization and the choice of basis in which H is truncated. Two broad categories within the Hamiltonian truncation methods are the Truncated Conformal Space Approach [4] and Discrete Light Cone Quantization [5]. A less traveled route consists in using the Fock-Space basis to truncate the Hamiltonian [1, 2, 6–10]. Lately there have been many advances in the Hamiltonian Truncation methods, see for instance [3, 11–17].

We review the truncated Hamiltonian approach following the discussion of ref. [1, 3]. The problem we are interested in is finding the spectrum of a strongly coupled QFT. Therefore we want to solve the eigenvalue equation

$$H|\mathcal{E}\rangle = \mathcal{E}|\mathcal{E}\rangle, \tag{1.1}$$

where $H = H_0 + V$, H_0 is a solvable Hamiltonian or the free Hamiltonian and V is the potential. H_0 is diagonalized by the states $H_0|E_n\rangle = E_n|E_n\rangle$. Suppose we are interested in studying the lowest energy states of the theory. One way to do it is separating the Hilbert space $\mathcal{H}$ into $\mathcal{H} = \mathcal{H}_l \oplus \mathcal{H}_h$, where $\mathcal{H}_l$ is of finite dimension and it is spanned by the states $|E_n\rangle$ with $E_n \leq E_T$. Then, the Hilbert space $\mathcal{H}_h$ is an infinite-dimensional Hilbert space containing the rest of the states $E_n > E_T$. The states are projected as $P_l|x\rangle \equiv |x_l\rangle \in \mathcal{H}_l$ and $(\mathbb{I} - P_l)|x\rangle = P_h|x\rangle \equiv |x_h\rangle \in \mathcal{H}_h$. Then, the eigenvalue problem can be replaced by

$$H_{\text{eff}}(\mathcal{E})|\mathcal{E}_l\rangle = \mathcal{E}|\mathcal{E}_l\rangle, \tag{1.2}$$

where $H_{\text{eff}} \equiv H_T + \Delta H(\mathcal{E})$, the truncated Hamiltonian is $H_T = P_l H P_l$ and

$$\Delta H(\mathcal{E}) = V_{lh} \frac{1}{\mathcal{E} - H_{0\,hh} - V_{hh}} V_{hl}, \tag{1.3}$$

with $O_{ij} \equiv P_i O P_j$ for $i, j \in \{h, l\}$. To derive eq. (1.2), project eq. (1.1) into the two equations

$$H_{ll}|\mathcal{E}_l\rangle + H_{lh}|\mathcal{E}_h\rangle = \mathcal{E}|\mathcal{E}_l\rangle, \qquad H_{hl}|\mathcal{E}_l\rangle + H_{hh}|\mathcal{E}_h\rangle = \mathcal{E}|\mathcal{E}_h\rangle, \tag{1.4}$$

and then substitute $|\mathcal{E}_h\rangle = (\mathcal{E} - H_{hh})^{-1} H_{hl}|\mathcal{E}_l\rangle$ from the second equation in (1.4) into the first.

Notice that eq. (1.2) is an exact equation and that a complete knowledge of $\Delta H(\mathcal{E})$ would render the original eigenvalue problem of eq. (1.1) solvable by an easy numerical diagonalization. In the limit where $E_T \to \infty$ the corrections ΔH to H_T can be neglected, but it is computationally very costly to increase the size of H_T and then diagonalize it. Therefore it is interesting to calculate ΔH to improve the numerical accuracy for a given E_T. A first step to compute ΔH is to perform an expansion of eq. (1.2) in powers of $V_{hh}(\mathcal{E} - H_0)^{-1}$,

$$\Delta H(\mathcal{E}, E_T) = \sum_{n=0}^{\infty} \Delta H_n(\mathcal{E}, E_T), \quad \text{where} \quad \Delta H_n(\mathcal{E}, E_T) = V_{lh} \frac{1}{\mathcal{E} - E_{hh}} \left(V_{hh} \frac{1}{\mathcal{E} - E_{hh}} \right)^n V_{hl},$$

where the matrix elements of ΔH_n are given by

$$\Delta H_n(\mathcal{E})_{rs} = \sum_{j_1,\cdots,j_{n-1}: E_{j_i}>E_T} V_{rj_1} \frac{1}{\mathcal{E}-E_{j_1}} V_{j_1j_2} \frac{1}{\mathcal{E}-E_{j_2}} V_{j_2j_3} \cdots V_{j_{n-2}j_{n-1}} \frac{1}{\mathcal{E}-E_{j_{n-1}}} V_{j_{n-1}s}\,,$$

(1.5)

in the H_0 eigenbasis and the sums run over all labels $j_1, \ldots, j_{n-1}$ of states belonging to $\mathcal{H}_h$ with r, s denoting the matrix elements (corresponding to eigenstates of H_0 with $E_s, E_r \leq E_T$ eigenvalues). Naively the truncation of the series in eq. (1.5) is justified for $V_{hh}/H_{0\,hh} < 1$ which for large enough E_T and $\mathcal{E} \ll E_T$ is fulfilled, and allows to go to strong coupling. This is discussed in detail in section 5.3. The operator ΔH depends on the exact eigenvalue and in practice the way eq. (1.2) is solved is by diagonalizing iteratively $H_{\text{eff}}(\mathcal{E}^*)$ starting with an initial seed $\mathcal{E}^*$. It is convenient to take $\mathcal{E}^*$ close to the exact eigenvalue $\mathcal{E}$, a simple and effective choice is to take the eigenvalue obtained from diagonalizing H_T.

In ref. [1] the ϕ^4 theory in two dimensions was studied at strong coupling using the Hamiltonian truncation method just presented in the Fock basis. There, the leading terms of ΔH_2 doing a local expansion were computed and shown to improve the results with respect to the ones found by only diagonalizing H_T. The main result of our work is to explain a way to calculate the exact corrections to ΔH at any order ΔH_n. As an example we calculate the ΔH_2 correction and some of the ΔH_3 terms for the ϕ^4 theory in two dimensions and present various approximation schemes for a faster numerical implementation. This can be seen as an extension of the method presented in ref. [1] which we believe to be very promising.

The paper is organized as follows. In section 2 we introduce a general formula to compute $\Delta H_n(\mathcal{E}, E_T)$ at any order n. Then we apply the method to the ϕ^2 and ϕ^4 scalar field theories in $d = 2$ space-time dimensions which we first define in section 3. The method is tested in section 4 by studying the spectrum of the solvable ϕ^2 perturbation with the calculation of ΔH_2 and ΔH_3. Other numerical tests are also performed in this section. Next, in section 5 we give the ΔH_2 correction for the ϕ^4 theory, and discuss the ΔH_3 calculation with some examples. There we also discuss the convergence of the ΔH_n expansion and compute the lowest energy levels of the theory at strong coupling. In section 6, we conclude and outline future directions of the method that are left open. In appendix A we introduce a simple diagrammatic representation to compute ΔH_n. Lengthy derivations and results are relegated to the appendices B and C. All the numerical calculations for this work have been done with `Mathematica`.

2 Calculation of ΔH at any order

In this section we present one of the main results of this paper which is the derivation of the nth-order correction ΔH_n of eq. (1.5) to the Truncated Hamiltonian. We start by defining the operator

$$\Delta \widehat{H}(\mathcal{E}) = \sum_{n=2}^{\infty} \Delta \widehat{H}_n(\mathcal{E}), \quad \text{where} \quad \Delta \widehat{H}_n(\mathcal{E}) = \left(V \frac{1}{\mathcal{E}-H_0} \right)^{n-1} V$$

(2.1)

which in the H_0 eigenbasis is given by

$$\Delta\widehat{H}_n(\mathcal{E})_{rs} = \sum_{j_1, \dots, j_{n-1}=1}^{\infty} V_{rj_1} \frac{1}{\mathcal{E} - E_{j_1}} V_{j_1 j_2} \frac{1}{\mathcal{E} - E_{j_2}} V_{j_2 j_3} \cdots V_{j_{n-2} j_{n-1}} \frac{1}{\mathcal{E} - E_{j_{n-1}}} V_{j_{n-1} s}\,,$$

(2.2)

where the indices $j_1, j_2, \dots, j_{n-1}$ run over the states of the full Hilbert space $\mathcal{H}$. Notice that the only difference between ΔH_n and $\Delta\widehat{H}_n$ is that the later receives contributions from all the eigenstates of H_0 while ΔH_n only from those with E_j energies $E_j > E_T$. This translates into the fact that each term in $\Delta H_n(\mathcal{E})$ has all the poles located at $\mathcal{E} > E_T$ as seen in eq. (1.5).

From here the derivation of ΔH_n follows from the observation that eq. (2.2) can be rewritten as the improper Fourier transform of the product of potentials restricted to positive times

$$\Delta\widehat{H}_n(\mathcal{E})_{rs} = \lim_{\epsilon \to 0} (-i)^{n-1} \int_0^\infty dt_1 \cdots dt_{n-1}\, e^{i(\mathcal{E} - E_r + i\epsilon)(t_1 + \cdots t_{n-1})}\, \mathcal{T}\{V(T_1) \cdots V(T_n)\}_{rs}\,,$$

(2.3)

where $T_k = \sum_{i=1}^{i=n-k} t_i$, $V(t) = e^{iH_0 t} V e^{-iH_0 t}$ and $\mathcal{T}$ denotes the time ordering operation.[1] Then, our method consists in applying the Wick theorem to eq. (2.3) to calculate $\Delta\widehat{H}_n$ and obtaining ΔH_n by keeping only the terms of $\Delta\widehat{H}_n$ corresponding to states with $E_j > E_T$, i.e. by keeping only the terms of $\Delta\widehat{H}_n$ which have all poles above E_T.[2] In the following sections we show how to carry this procedure for the cases of the ϕ^2 perturbation and ϕ^4 theory.

3 Scalar theories

We study scalar theories in two space-time dimensions defined by the Minkowskian action $S = S_0 + S_I$ where

$$S_0 = \frac{1}{2} \int_{-\infty}^{\infty} dt \int_0^L dx\, :(\partial\phi)^2 - m^2\phi^2:\,,$$

(3.1)

$$S_I = -\int_{-\infty}^{\infty} dt\, V(\phi) = -g_\alpha \int_{-\infty}^{\infty} dt \int_0^L dx\, :\phi^\alpha:\,.$$

(3.2)

For simplicity we consider the cases where $\alpha = 2, 4$ and $m^2 > 0$. The symbol $::$ stands for normal ordering which for S_0 means that we set the vacuum energy to zero; while the interaction term is normal ordered with respect to S_0, which in perturbation theory is

---

[1] This can be seen by introducing the indentity $\mathbb{I} = \sum_n |E_n\rangle\langle E_n|$ between each pair of V's in eq. (2.3) and integrating over all times $t_1, \dots t_n$. Also notice that the time ordering operation is trivial because the V operators are time ordered in all the integration domain. The $\lim_{\epsilon \to 0}$ is taken at the end of the calculation.

[2] This procedure can be formalized as follows. The first correction can be written as $\Delta H_2(\mathcal{E}) = \int_\mathcal{C} \frac{dz}{2\pi i} \frac{\Delta\widehat{H}_2(z)}{\mathcal{E} - z}$, where $\mathcal{C}$ is any path than encircles only all the poles above E_T. For $\Delta H_3(\mathcal{E}) = \int_\mathcal{C} \frac{dz}{2\pi i} \frac{1}{\mathcal{E} - z} \int_\mathcal{C} \frac{dz'}{2\pi i} \frac{1}{\mathcal{E} - z'} \Delta\widehat{H}_3(z', z)$ where we have generalized the operator $\Delta\widehat{H}_3(z, z')_{rs} = -\lim_{\epsilon \to 0} \int_0^\infty dt_1 dt_2\, e^{i(z - E_r + i\epsilon)t_1} e^{i(z' - E_r + i\epsilon)t_2}\, \mathcal{T}\{V(T_1)V(T_2)V(T_3)\}_{rs}$. The generalization to the nth correction is straightforward.

equivalent to renormalize to zero the UV divergences from closed loops with propagators starting and ending on the same vertex.

To study these theories using the Hamiltonian truncation method we begin by defining them on the cylinder $\mathbb{R} \times S_1$ where the circle corresponds to the space direction which we take to have a length $Lm \gg 1$, and $\mathbb{R}$ is the time. We impose periodic boundary conditions $\phi(t, x) = \phi(t, x + nL)$ for $n \in \mathbb{Z}$ on S_1. The compact space direction makes the spectrum of the free theory discrete and regularizes the infra-red (IR) divergences.

In canonical quantization the scalar operators can be expanded in terms of creation and annihilation operators as

$$\phi(x) = \sum_k \frac{1}{\sqrt{2L\omega_k}} \left(a_k e^{ikx} + a_k^\dagger e^{-ikx} \right), \tag{3.3}$$

where $\omega_k = \sqrt{m^2 + k^2}$, $k = \frac{2\pi n}{L}$ with $n \in \mathbb{Z}$ and the creation and anihilation operators satisfy the commutation relations

$$\left[a_k, a_{k'}^\dagger \right] = \delta_{kk'}, \qquad \left[a_k, a_{k'} \right] = 0. \tag{3.4}$$

The Hamiltonian then reads $H = H_0 + V$, where

$$H_0 = \sum_k \omega_k \, a_k^\dagger a_k \tag{3.5}$$

and the potentials for a ϕ^2 and a ϕ^4 interaction are given by

$$V = g_2 \sum_{k_1 k_2} \frac{L \, \delta_{k_1 + k_2, 0}}{\sqrt{2L\omega_{k_1}} \sqrt{2L\omega_{k_2}}} \left(a_{k_1} a_{k_2} + a_{-k_1}^\dagger a_{k_2} \right) + \text{h.c.}, \tag{3.6}$$

and

$$V = g \sum_{k_1, k_2, k_3, k_4} \frac{L \, \delta_{\sum_{i=1}^4 k_i, 0}}{\prod_{i=1}^4 \sqrt{2L\omega_{k_i}}} \left(a_{k_1} a_{k_2} a_{k_3} a_{k_4} + 4 a_{-k_1}^\dagger a_{k_2} a_{k_3} a_{k_4} + 3 a_{-k_1}^\dagger a_{-k_2}^\dagger a_{k_3} a_{k_4} \right) + \text{h.c.}, \tag{3.7}$$

respectivley, where $g \equiv g_4$ and $\delta_{k_1 + k_2, 0}$, $\delta_{\sum_{i=1}^4 k_i, 0}$ stand for Kronecker deltas.

We implement the Hamiltonian truncation using the basis of H_0 eigenstates

$$| E_i \rangle = \frac{a_{k_N}^{\dagger \, n_N}}{\sqrt{n_N!}} \cdots \frac{a_{k_2}^{\dagger \, n_2}}{\sqrt{n_2!}} \frac{a_{k_1}^{\dagger \, n_1}}{\sqrt{n_1!}} | 0 \rangle. \tag{3.8}$$

which satisfy $\mathbb{I} = \sum_i | E_i \rangle \langle E_i |$, where $E_i = \sum_{s=1}^N n_s \sqrt{k_s^2 + m^2}$ and $H_0 | 0 \rangle = 0$. The Hilbert space is divided into $\mathcal{H} = \mathcal{H}_l \oplus \mathcal{H}_h$ with $\mathcal{H}_l$ spanned by the states $| E_r \rangle$ such that $E_i \leq E_T$ while $\mathcal{H}_h$ is spanned by the rest of the basis. Then, the truncated Hamiltonian is

$$(H_T)_{rs} = \langle E_r | H | E_s \rangle, \quad \text{for} \quad E_i \leq E_T. \tag{3.9}$$

In this basis, the operator ΔH is given by

$$\Delta H(\mathcal{E})_{rs} = \sum_{j, j'} V_{rj} \left(\frac{1}{\mathcal{E} - H_0 - V} \right)_{jj'} V_{j's} \tag{3.10}$$

where the labels r, s denote entries with $E_r, E_s \leq E_T$ and the sum over j, j' runs over all states with $E_j, E_{j'} > E_T$.

The Hamiltonian H can be diagonalized by sectors with given quantum numbers associated with operators that commute with H. These are the total momentum P, the spatial parity $\mathcal{P} : x \rightarrow -x$ and the field parity $\mathbb{Z}_2 : \phi(x) \rightarrow -\phi(x)$, which act on the H_0-eigenstates as $P | E_i \rangle = \sum_s n_s k_s | E_i \rangle$, $\mathcal{P} \prod_{i=1}^N \frac{a_{k_i}^{\dagger \, n_i}}{\sqrt{n_i!}} | 0 \rangle = \prod_{i=1}^N \frac{a_{-k_i}^{\dagger \, n_i}}{\sqrt{n_i!}} | 0 \rangle$ and $\mathbb{Z}_2 | E_i \rangle = (-1)^{\sum_s n_s} | E_i \rangle$. We work in the orthonormal basis of eigenstates of H_0, P, $\mathcal{P}$ and $\mathbb{Z}_2$ given by

$$| \widetilde{E}_i \rangle = \beta \cdot \left(| E_i \rangle + \mathcal{P} | E_i \rangle \right), \tag{3.11}$$

where $\beta = 1/2, \, 1/\sqrt{2}$ for $\mathcal{P} | E_i \rangle = | E_i \rangle$ and $\mathcal{P} | E_j \rangle \neq | E_j \rangle$, respectively. As done in ref. [1], in the whole paper we focus on the sub-sector with total momentum $P | \widetilde{E}_i \rangle = 0$, spatial parity $\mathcal{P} | \widetilde{E}_i \rangle = + | \widetilde{E}_i \rangle$ and diagonalize separately the $\mathbb{Z}_2 = \pm$ sectors.[3] In this paper we do not investigate the dependence of the spectrum as a function of the length L of the compact dimension which we leave for future work, and always consider it to be finite.[4] All the numerical calculations are done for $m = 1$ and $L = 10$.

4 Case study ϕ^2 perturbation

In this section we apply the method introduced in section 2 to the scalar theory $H = H_0 + V$ with a potential

$$V = g_2 \int_0^L dt \; : \phi^2 : \tag{4.1}$$

This is a simple theory that allows to illustrate various aspects of the calculation of $\Delta \widehat{H}$ in eq. (2.3) and its relation to ΔH. Also since the theory is solvable we can compare our procedure with the exact results. The theory is solved by using the eigenstates of H, given by

$$| \mathcal{E}_i \rangle = \frac{b_{k_N}^{\dagger \, n_N}}{\sqrt{n_N!}} \cdots \frac{b_{k_2}^{\dagger \, n_2}}{\sqrt{n_2!}} \frac{b_{k_1}^{\dagger \, n_1}}{\sqrt{n_1!}} | \Omega \rangle, \tag{4.2}$$

where $| \Omega \rangle = | \mathcal{E}_0 \rangle$ is the vacuum of the theory and $b^\dagger / b$ are the creation/annihilation operators so that

$$H = \sum_k b_k^\dagger b_k \Omega_k + \mathcal{E}_0, \tag{4.3}$$

with $\Omega_k = \sqrt{\omega_k^2 + 2g_2}$. Then, one can relate the operators $b^\dagger / b$ to the $a^\dagger / a$ in H_0 (given in eq. (3.5) and eq. (3.6)) by the Bogolyubov transformation $b_k = \sinh \alpha_k \, a_{-k}^\dagger + \cosh \alpha_k \, a_k$ provided that $\Omega_k \sinh 2\alpha_k = \omega_k^{-1} g_2$, $\Omega_k \cosh 2\alpha_k = \omega_k + g_2/\omega_k$. Then, since $\langle 0 | H | 0 \rangle = 0$

---

[3]For the $V = \int dt \, : \phi^2 :$ theory, the matrix element $\langle E_i | V | E_j \rangle = 0$ with $\mathcal{P} | E_i \rangle = | E_i \rangle$ and $\mathcal{P} | E_j \rangle \neq | E_j \rangle$. Therefore, one can diagonalize the $\mathcal{P} | E_i \rangle = | E_i \rangle$ and $\mathcal{P} | E_i \rangle \neq | E_i \rangle$ sectors separately.

[4]To match the $L \rightarrow \infty$ spectrum one has to take into account the Casimir energy difference between the $L \rightarrow \infty$ and the finite L theory and inspect how various states converge as L is increased. See refs. [18, 19] and ref. [1] for a thorough study of the L dependence.

we have that [1]:

$$\mathcal{E}_0(g_2) = \frac{1}{2} \sum_k \left(\sqrt{\omega_k^2 + 2g_2} - \omega_k - \frac{g_2}{\omega_k} \right) = \frac{L(m^2 + 2g_2)}{8\pi} \left[\log \left(\frac{m^2}{m^2 + 2g_2} \right) + \frac{2g_2}{m^2 + 2g_2} \right], \tag{4.4}$$

where the sum can be done by means of the Abel-Plana formula, which is the exact vacuum energy of the theory.

A brief summary of the rest of this section is the following. In section 4.1 and section 4.2 we calculate the 2 and 3-point corrections to the operator ΔH. In section 4.3 we perform a numerical test to check that our expressions for ΔH are correct. Then, in section 4.4 we discuss the numerical results and the convergence of the expansion $\Delta H(\mathcal{E}_i) = \sum_n \Delta H_n(\mathcal{E}_i)$ by comparing with the exact spectrum $\mathcal{E}_i$.

4.1 Two-point correction

Following the steps explained in section 2 we begin the calculation of the two-point correction by first computing $\Delta \widehat{H}_2$. From eq. (2.3) we have that

$$\Delta \widehat{H}_2(\mathcal{E})_{rs} = \sum_j V_{rj} \frac{1}{\mathcal{E} - E_j} V_{js} = \lim_{\epsilon \to 0} -i \int_0^\infty dt\, e^{i(\mathcal{E} - E_r + i\epsilon)t} \mathcal{T}\{V(t)V(0)\}_{rs}. \tag{4.5}$$

Then, applying the Wick theorem to eq. (4.5) we find

$$\lim_{\epsilon \to 0} -ig_2^2 \int_0^\infty dt\, e^{i(\mathcal{E} - E_r + i\epsilon)t} \int_{-L/2}^{L/2} dx dz \sum_{m=0}^2 s_{2-m} D_F^{2-m}(z,t) : \phi^m(x+z,t)\phi^m(x,0) :_{rs}, \tag{4.6}$$

where $s_p = \binom{2}{p}^2 p!$ are the symmetry factors and $D_F(z,t)$ is the Feynman propagator with discretized momenta. Henceforth we label the terms $m = 0, 1, 2$ by $\Delta \widehat{H}_2^{\phi^{2m}}$ so that $\Delta \widehat{H}_2 = \Delta \widehat{H}_2^{\mathbb{1}} + \Delta \widehat{H}_2^{\phi^2} + \Delta \widehat{H}_2^{\phi^4}$ and similarly for ΔH_2; the labels only inform about the total number of fields in each term which do not need to be local. Due to the time integration domain, it is convenient to use *half* Feynman propagator

$$D_L(z,t) \equiv D_F(z,t)\theta(t) = \frac{1}{2L} \sum_{n=-\infty}^{n=\infty} \frac{1}{\omega_k} e^{-i\omega_k t} e^{i\frac{2\pi nz}{L}} \theta(t), \tag{4.7}$$

the momentum of the propagator is discretised due to the finite extent of the space. Next, we proceed to calculate the operators in eq. (4.6), starting with the detailed calculation of the coefficient of the identity operator $\Delta \widehat{H}_2^{\mathbb{1}}$:

$$\Delta \widehat{H}_2^{\mathbb{1}}(\mathcal{E})_{rs} = \lim_{\epsilon \to 0} -is_2 g_2^2 \int_0^\infty dt \int_{-L/2}^{L/2} dz\, e^{i(\mathcal{E} - E_r + i\epsilon)t_1} D_L^2(t,z) \mathbb{1}_{rs}, \tag{4.8}$$

where $\mathbb{1}_{rs} \equiv \delta_{rs} \int_{-L/2}^{L/2} dz$ has dimensions of $[E]^{-1}$. Then, upon inserting the propagator of eq. (4.7) and performing the space-time integrals we find

$$\Delta \widehat{H}_2^{\mathbb{1}}(\mathcal{E})_{rs} = \frac{s_2 g_2^2}{4L} \sum_k \frac{1}{\omega_k^2} \frac{1}{\mathcal{E} - E_r - 2\omega_k} \mathbb{1}_{rs}. \tag{4.9}$$

The operator in eq. (4.9) has poles from all possible intermediate states and, as explained in section 2, the operator $\Delta H_2^{\mathbb{1}}(\mathcal{E})$ is found by keeping only those terms with poles located at $E_r + 2\omega_k > E_T$, therefore

$$\Delta H_2^{\mathbb{1}}(\mathcal{E})_{rs} = \frac{s_2 g_2^2}{L} \sum_{k: E_r+2\omega_k>E_T} \frac{1}{4\,\omega_k^2} \frac{1}{\mathcal{E} - E_r - 2\omega_k}\, \mathbb{1}_{rs}\,. \tag{4.10}$$

The calculations of $\Delta H_2^{\phi^2}$ is similar to the one for eq. (4.10), we start by computing

$$\Delta \widehat{H}_2^{\phi^2}(\mathcal{E})_{rs} = \lim_{\epsilon \to 0} -is_1 g_2^2 \int_0^\infty dt \int_{-L/2}^{L/2} dx dz\, e^{i(\mathcal{E}-E_r+i\epsilon)t_1} D_L(z,t) : \phi(x+z,t)\phi(x,0):_{rs}, \tag{4.11}$$

where we expand $:\phi(x+z,t)\phi(x,0):$ in modes, as in eq. (3.3), and do the simple space-time integrals. For the full expressions of $\Delta \widehat{H}_2^{\phi^2}$ see appendix B. Then, keeping only the terms with poles at $\mathcal{E} > E_T$ we get

$$\Delta H_2^{\phi^2}(\mathcal{E})_{rs} = s_1 g_2^2 \sum_{q: 2\omega_q+E_r>E_T} \frac{1}{4\,\omega_q^2} \frac{1}{\mathcal{E} - E_r - 2\omega_q} \left(a_q^\dagger a_q\right)_{rs}. \tag{4.12}$$

The operator $\Delta H_2^{\phi^4}$ is obtained in a similar way,

$$\Delta H_2^{\phi^4}(\mathcal{E})_{rs} = s_0 g_2^2 \sum_{q_1,q_2: 2\omega_{q_2}+E_r>E_T} \frac{1}{4\,\omega_{q_2}\omega_{q_1}} \frac{1}{\mathcal{E} - E_r - 2\omega_{q_2}} \left(a_{q_1}^\dagger a_{-q_1}^\dagger a_{q_2} a_{-q_2}\right)_{rs}. \tag{4.13}$$

In appendix A we give a simple way to derive these expressions from diagrams, and for the full expressions of $\Delta \widehat{H}_2^{\phi^2}$ and $\Delta \widehat{H}_2^{\phi^4}$ see appendix B. Notice that the values of q_1, q_2 and q appearing in the sums of eq. (4.12) and eq. (4.13) can take only the momenta of the states $|E_s\rangle \in \mathcal{H}_l$ on which a and $a^\dagger$ act, and therefore are bounded. On the other hand, the values of the k's in eq. (4.10) go all the way to infinity. Also, even though the operators in eq. (4.12) and eq. (4.13) may seem not hermitian due to the E_r appearing in the expressions, one can see that the operator $(\Delta H_2^{\phi^2})_{rs}$ is diagonal and therefore $E_r = E_s$, while $\Delta H_2^{\phi^4}$ is not diagonal, but one can check that $E_r + 2\omega_{q_2} = E_s + 2\omega_{q_1}$, making it hermitian as well.

We end this section by noticing that the operator of eq. (4.10) can be rewritten as

$$(\Delta H_2^{\mathbb{1}})_{rs} = \int_{E_T}^\infty \frac{dE}{\mathcal{E} - E} \frac{s_2 g_2^2}{L} \sum_{k=-\infty}^\infty \frac{\delta(E - E_r - 2\omega_k)}{(2\omega_k)^2}\, \mathbb{1}_{rs} = s_2 g_2^2 \int_{E_T}^\infty \frac{dE}{2\pi} \frac{\Phi_2(E - E_r)}{\mathcal{E} - E}\, \mathbb{1}_{rs}\,, \tag{4.14}$$

where Φ_2 is the two-particle phase space with discretized momenta,

$$\Phi_2(E - E_r) = \sum_{k_1,k_2} \frac{L\,\delta_{k_1+k_2,0}}{(2L\omega_{k_1})(2L\omega_{k_2})}\, 2\pi\,\delta(E - E_r - \omega_{k_1} - \omega_{k_2})\,, \tag{4.15}$$

where from eq. (4.14) one has that $E - E_r > 2m$.[5] Eq. (4.14) can be evaluated by means of the Abel-Plana formula, which for $LE_T \gg 1$ is well approximated by its continuum limit.[6]

---

[5]The lower limit in eq. (4.14) should be taken slightly above E_T to reproduce the lower limit q: $2\omega_q + E_r > E_T$ in the sum of eq. (4.9).

[6]The difference between the continuum limit and discrete result ranges from $\mathcal{O}(g^2 L^{-1} E_T^{-3})$ to $\mathcal{O}(g^2 L^{-1} E_T^{-1} m^{-2})$ depending on the matrix entry.

The continuum two-body phase space is given by

$$\Phi_2(E) = \int_{-\infty}^{\infty} \frac{d^2p_1}{(2\pi)^2 \, 2\omega_{p_1}} \frac{d^2p_2}{(2\pi)^2 \, 2\omega_{p_2}} (2\pi)^2 \, \delta^{(2)}(P^\mu - p_1 - p_2) = \frac{1}{E\sqrt{E^2 - 4m^2}}\,, \quad (4.16)$$

where $P^\mu = (E, 0)$ and $E > 2m$. Therefore (for $LE_T \gg 1$) we find

$$\Delta H_2^{\mathbb{1}}(\mathcal{E})_{rs} \simeq s_2 g_2^2 \int_{E_T}^{\infty} \frac{dE}{2\pi} \frac{1}{\mathcal{E} - E} \frac{1}{E - E_r} \frac{1}{\sqrt{(E - E_r)^2 - 4m^2}} \, \theta(E - E_r - 2m) \, \mathbb{1}_{rs}\,. \quad (4.17)$$

This result is useful for numerical implementation since eq. (4.17) can be integrated in terms of logarithmic functions. Finally, we notice that upon expanding the function $s_2/(2\pi)\Phi_2(E)$ around $m/E = 0$ we find agreement with ref. [1] that computed it by other means (there called $\mu_{220}(E) = 1/(\pi E^2)$).

4.2 Three-point correction

The calculation of the three-point correction ΔH_3 also starts from the expression in eq. (2.3)

$$\Delta \widehat{H}_3(\mathcal{E})_{rs} = -\lim_{\epsilon \to 0} \int_0^{\infty} dt_1 dt_2 \, e^{i(\mathcal{E} - E_r + i\epsilon)(t_1 + t_2)} \mathcal{T}\{V(T_1)V(T_2)V(T_3)\}_{rs}\,, \quad (4.18)$$

where $T_k = \sum_{n=1}^{3-k} t_n$. Next we apply the Wick theorem and find that the time ordered product $\mathcal{T}\{V(T_1)V(T_2)V(T_3)\}$ is given by

$$g_2^3 \int_{-L/2}^{L/2} dx_1 dx_2 dz \sum_{m,n,v=0}^{2} s_2^{mnv} D_F^m(x_1, t_1) D_F^n(x_2, t_2) D_F^v(x_1 + x_2, t_1 + t_2) : \phi_{X_1, T_1}^{2-n-m} \phi_{X_2, T_2}^{2-n-v} \phi_{X_3, T_3}^{2-v-m} : \quad (4.19)$$

where we have introduced the notation $X_k = z + \sum_{n=1}^{3-k} x_n$ and $\phi_{x,t} = \phi(x,t)$; while the symmetry factor is given by

$$s_p^{mnv} = \frac{p!^3}{(p - m - n)!(p - m - v)!(p - n - v)!m!n!v!}\,. \quad (4.20)$$

We use the same notation as in the previous section $\Delta \widehat{H}_3 = \Delta \widehat{H}_3^{\mathbb{1}} + \Delta \widehat{H}_3^{\phi^2} + \Delta \widehat{H}_3^{\phi^4} + \Delta \widehat{H}_3^{\phi^6}$, and similarly for ΔH_3. Then, upon performing the space-time integrals in eq. (4.19) and only keeping the terms with all the poles above E_T we find ΔH_3. Then, for the term $\Delta H_3^{\mathbb{1}}$ we get

$$\Delta H_3^{\mathbb{1}}(\mathcal{E})_{rs} = s_2^{111} g_2^3 \frac{1}{L} \sum_{k:\, E_{rs} + 2\omega_k > E_T} \frac{1}{(2\omega_k)^3} \frac{1}{(\mathcal{E} - E_r - 2\omega_k)^2} \, \mathbb{1}_{rs}\,. \quad (4.21)$$

The expressions for $\Delta H_3^{\phi^2}$, $\Delta H_3^{\phi^4}$ and $\Delta H_3^{\phi^6}$ are lengthy but straightforward to obtain and are relegated to appendix B.

As done in the previous section, eq. (4.21) can be written as

$$\Delta H_3^{\mathbb{1}}(\mathcal{E})_{rs} = s_2^{111} g_2^3 \int_{E_T}^{\infty} \frac{dE}{(\mathcal{E} - E)^2} \frac{1}{L} \sum_k \frac{1}{(2\omega_k)^3} \delta(E - E_r - 2\omega_k) \, \mathbb{1}_{rs}\,, \quad (4.22)$$
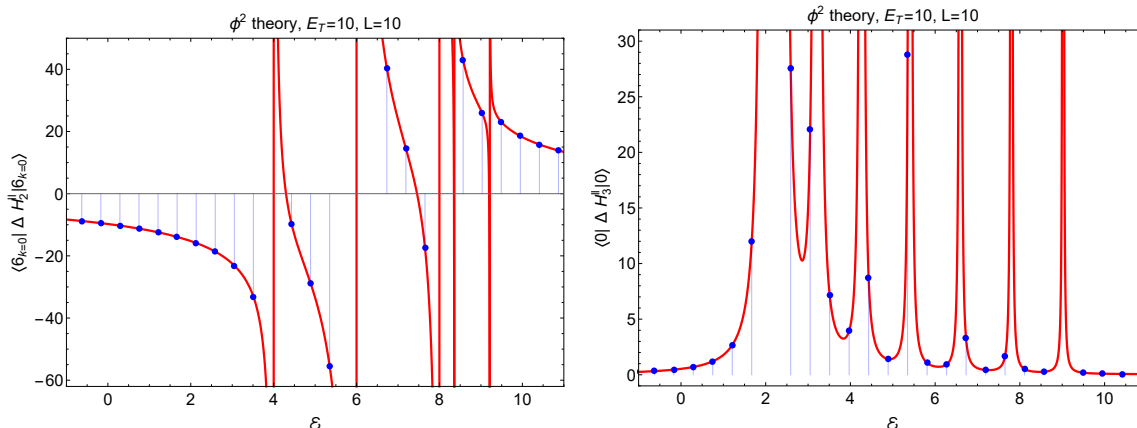
– 9 –

Figure 1. Comparison of both sides of eqs. (4.24) and (4.25).

which for $L^{-1}E_T \gg 1$ is well approximated by its continuum limit

$$\Delta H_3^1(\mathcal{E})_{rs} \simeq s_2^{111} \frac{g_2^3}{2\pi} \int_{E_T}^{\infty} \frac{dE}{(\mathcal{E} - E)^2} \frac{1}{(E - E_r)^2} \frac{1}{\sqrt{(E - E_r)^2 - 4m^2}} \mathbb{1}_{rs}, \qquad (4.23)$$

and can be integrated in terms of logarithmic functions. This is useful for a fast numerical implementation.

4.3 A numerical test

We perform a numerical check to test our prescription to select the poles of $\Delta \widehat{H}_n(\mathcal{E})$ to get ΔH_n, i.e. that we can select the desired intermediate states of H_0 by looking at the poles of the terms of $\Delta \widehat{H}_n$. The check consists in computing $\Delta \widehat{H}_2$ as explained, and then selecting only the terms with all poles at $\mathcal{E} \leq E_T$. We refer to the expression as ΔH_n^{ll} to differentiate it with ΔH_n that only receives corrections from terms with poles at $\mathcal{E} > E_T$. ΔH_2^{ll} is then compared with the matrix elements of $V P_l (\mathcal{E} - H_0)^{-1} P_l V$, finding an exact agreement. The same is done for $\Delta \widehat{H}_3(\mathcal{E})$ by comparing it against $V P_l (\mathcal{E} - H_0)^{-1} V (\mathcal{E} - H_0)^{-1} P_l V$. This check has been done for all the matrices used in the present work, both for ϕ^2 and ϕ^4. For brevity we only show the check for two matrix entries of the ϕ^2 theory. These are

$$\langle 6_{k=0} | V P_l \frac{1}{\mathcal{E} - H_0} P_l V | 6_{k=0} \rangle = \sum_{k:\, 2\omega_k + 6m < E_T} \frac{g_2^2}{2\,\omega_k^2} \frac{1}{\mathcal{E} - 6m - 2\omega_k}$$
$$+ \frac{3\,g_2^2}{2m^2} \left(\frac{5}{\mathcal{E} - 4m} + \frac{24}{\mathcal{E} - 6m} + \frac{9}{\mathcal{E} - 8m} \right), \qquad (4.24)$$

$$\langle 0 | V P_l \frac{1}{\mathcal{E} - H_0} V \frac{1}{\mathcal{E} - H_0} P_l V | 0 \rangle = g_2^3 \sum_{k:\, 2\omega_k < E_T} \frac{1}{\omega_k^3} \frac{1}{(\mathcal{E} - 2\omega_k)^2}. \qquad (4.25)$$

In figure 1 we compare both sides of equations eq. (4.24) and (4.25). The red curves correspond to the right hand side of eqs. (4.24)–(4.25), which are our analytical results, and the blue dots are given by the product of the matrices in the left hand side of the equations. In the left plot, done for $\langle 6_{k=0} | \Delta H_2^{ll} | 6_{k=0} \rangle$, the first pole arises at the four-particle threshold and subsequent poles appear for higher excited states. Instead, the first
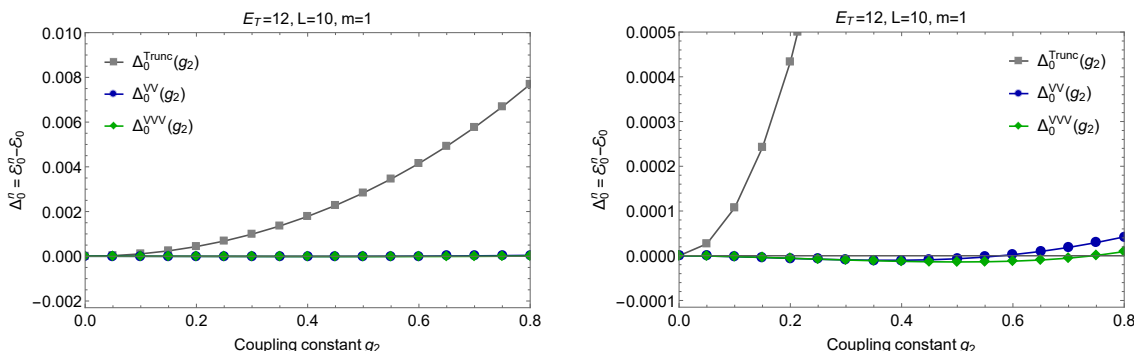
Figure 2. *Left*: comparison of the exact vacuum energy with the numerical result as a function of the coupling constant g_2 (for $V = g_2 \int dx \phi^2$). *Right*: left plot with the y-axis zoomed in a factor $\times 20$.

pole in the right plot, done for $\langle 0 | \Delta H_3^{ll} | 0 \rangle$, occurs at $\mathcal{E} = 2m$. Notice that in both figures there are no poles for $\mathcal{E} > E_T$.

4.4 Spectrum and convergence

We perform a numerical study of the convergence of the energy levels as a function of the truncation energy E_T and their convergence as higher order corrections ΔH_n are calculated for a fixed E_T. We use the formulas in eqs. (4.10)–(4.13), (4.21) and (B.5)–(B.8) to numerically compute ΔH_2 and ΔH_3.[7]

We begin by comparing the vacuum eigenstate $\mathcal{E}_0^i$ obtained by numerically diagonalizing $H_T + \sum_{n=2}^{N} \Delta H_n$ (for $N = 2$ and 3) with the exact vacuum energy $\mathcal{E}_0$. In figure 2 we show a plot of $\Delta_0^i = \mathcal{E}_0^i - \mathcal{E}_0$ as a function of the coupling constant g_2. The plot is done for a truncation energy of $E_T = 12$ and $L = 10$ (recall that we work in $m = 1$ units). For an easier comparison with previous work, these plots have been done with the same choice of parameters and normalizations as in figure 2 of ref. [1]. The gray curve in figure 2 is obtained by numerically diagonalizing H_T, whose lowest eigenvalue is $\mathcal{E}_0^{\mathrm{T}}$. The blue curve is obtained by diagonalizing the renormalized hamiltonian $H_T + \Delta H_2(\mathcal{E}_0^{\mathrm{T}})$, whose lowest eigenvalue is $\mathcal{E}_0^{VV}$. Lastly, the green curve is obtained by diagonalizing $H_T + \Delta H_2(\mathcal{E}_0^{VV}) + \Delta H_3(\mathcal{E}_0^{VV})$ (we find little difference in evaluating the latter operator in $\mathcal{E}_0^{\mathrm{Trunc}}$ instead of $\mathcal{E}_0^{VV}$). The right plot of figure 2 is a zoomed in version of the left plot in order to resolve the difference between the Δ_0^{VV} and Δ_0^{VVV} curves.

The right plot shows that overall Δ_0^{VVV} performs better than Δ_0^{VV}, this indicates that the truncation of the series expansion $\Delta H = \sum_{n=2}^{\infty} \Delta H_n$ at $n = 3$ is perturbative in the studied range. The effect is more pronounced for the highest couplings $g_2 \simeq [0.6, 0.8]$. As a benchmark value $\mathcal{E}_0(g_2 = 0.8) = -0.351864$, see eq. (4.4). Therefore the relative error at $g_2 = 0.8$ is 2%, 0.01% and 0.002% for the Truncated, the VV and the VVV corrections, respectively.

---

[7]The sums over k in eqs. (4.10)–(4.13), (4.21) and (B.5)–(B.8) have been done with a cutoff $k = 250$. We have checked that increasing the cutoff has little impact on the results and find agreement with analytic formulas like eq. (4.14).
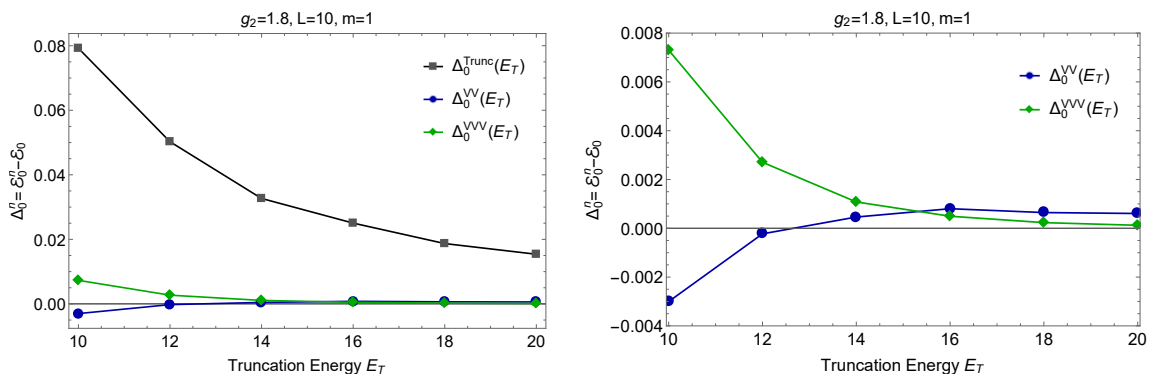
Figure 3. *Left*: comparison of the exact vacuum energy with the numerical result as a function of the truncation energy E_T. *Right*: left plot zoomed in.
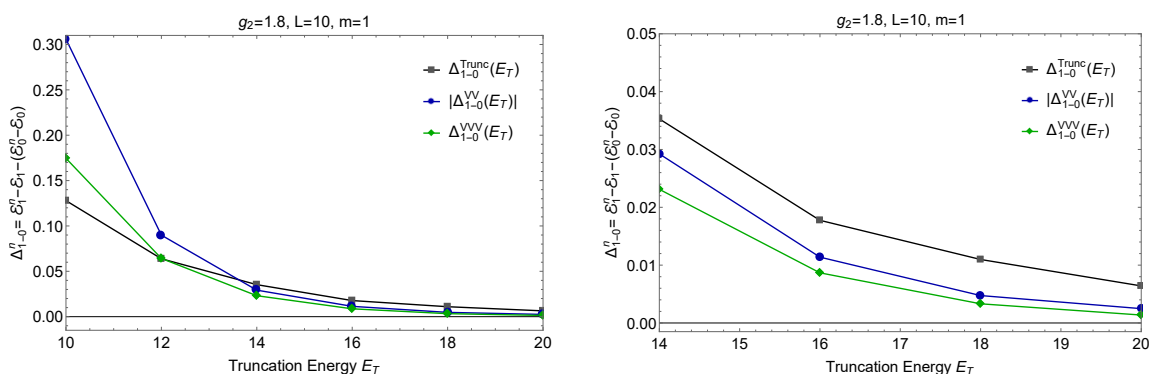

Figure 4. *Left*: comparison of the exact energy difference $\mathcal{E}_1 - \mathcal{E}_0$ with respect the numerical result as a function of the truncation energy E_T. *Right*: left plot zoomed in. On both plots we have taken the absolute value of the curve corresponding to the VV corrections, in blue.

Next, we check the convergence of the energy levels as a function of the truncation energy E_T. In figure 3, in the left plot we show $\Delta_0^i = \mathcal{E}_0^i - \mathcal{E}_0$ as a function of the truncation energy E_T, for $i =$ Trunc, VV and VVV. Both the Δ_0^{VV} and Δ_0^{VVV} curves give better results than Δ_0^{Trunc} for the whole range. Also, the curves Δ_0^{VV} and Δ_0^{VVV} have a better convergence behavior and, when converged, they are closer to zero than Δ_0^{Trunc}. The right plot is a zoomed in version to resolve the difference between Δ_0^{VV} and Δ_0^{VVV}. The plot shows that for $E_T \lesssim 15$ the curve Δ_0^{VV} gives better results than Δ_0^{VVV} while for larger E_T the behavior is reversed. This indicates that for $E_T \lesssim 15$ (and $g_2 = 1.8$) the truncation of the series $\Delta H = \sum_{n=2}^{\infty} \Delta H_n$ is not a good approximation, and adding more terms will not improve the accuracy. However, as E_T is increased it pays off to introduce higher order corrections to get a better result. This is because Δ_0^{VVV} has a faster converge rate than Δ_0^{VV} to the real eigenvalue. The value is $\mathcal{E}_0(g_2 = 1.8) = -1.360719$, see eq. (4.4). Therefore the relative error at $E_T = 20$ is 1%, 0.04% and 0.009% for the Truncated, the VV and the VVV corrections, respectively.

In figure 4 we repeat the plots of figure 3 for the first $\mathbb{Z}_2$-even excited state but taking the absolute value of the Δ_1^{VV} curve for clarity. The plots show a similar convergence rate

for the three Δ_1^i curves. However, there is a similar pattern compared to figure 3: for $E_T \lesssim 15$ introducing higher order corrections of the series $\Delta H = \sum_{n=2}^{\infty} \Delta H_n$ gives worse results, while for larger values of E_T adding higher ΔH_n corrections improves them. The value is $\mathcal{E}_1(g_2 = 1.8) = 0.784042$, hence the relative error at $E_T = 20$ is 0.8%, 0.3% and 0.17% for the Truncated, the VV and the VVV corrections, respectively.

5 The ϕ^4 theory

Next we apply the method presented in previous sections to the ϕ^4 theory. We start by deriving the exact expressions for ΔH_2 in detail, then we perform various useful approximations for a faster numerical implementation and discuss general aspects of the method. We also discuss the pertubativity of the ΔH_n expansion and compute the spectrum of the theory at different couplings while studying its behaviour in E_T and g using the results of ΔH_2. We end the section with some comments on future work and a discussion of the calculation of ΔH_3.

5.1 Two-point correction

Again, we follow section 2 to derive ΔH by first computing $\Delta \widehat{H}$. From eq. (2.3) we have

$$\Delta \widehat{H}_2(\mathcal{E})_{rs} = \sum_j V_{rj} \frac{1}{\mathcal{E} - E_j} V_{js} = \lim_{\epsilon \to 0} -i \int_0^{\infty} dt\, e^{i(\mathcal{E} - E_r + i\epsilon)t} \mathcal{T}\{V(t)V(0)\}_{rs}. \qquad (5.1)$$

It is convenient to re-write the two-point correction in the following equivalent form

$$\Delta \widehat{H}_2(\mathcal{E})_{rs} = \sum_j V_{rj} \frac{1}{\mathcal{E} - E_j} V_{js} = \lim_{\epsilon \to 0} -i \int_0^{\infty} dt\, e^{i(\mathcal{E} - E_{rs} + i\epsilon)t} \mathcal{T}\{V(t/2)V(-t/2)\}_{rs}, \qquad (5.2)$$

where $E_{rs} = (E_r + E_s)/2$. Applying the Wick theorem we find

$$-ig^2 \int_0^{\infty} dt\, e^{i(\mathcal{E} - E_{rs} + i\epsilon)t} \int_{-L/2}^{L/2} dx\, dz \sum_{m=0}^{4} s_{4-m} D_F^{4-m}(z,t) : \phi^m(x+z, t/2)\phi^m(x, -t/2) :_{rs}, \qquad (5.3)$$

where $s_p = \binom{4}{p}^2 p!$ are the symmetry factors. By integrating eq. (5.3) and keeping only the contributions from high energy intermediate states $E_j > E_T$ we obtain the exact expression for ΔH_2. We use the shorthand notation $\Delta H_2 = \Delta H_2^{\mathbb{1}} + \Delta H_2^{\phi^2} + \Delta H_2^{\phi^4} + \Delta H_2^{\phi^6} + \Delta H_2^{\phi^8}$ for $m = 0, 1, 2, 3, 4$, and similarly for $\Delta \widehat{H}_2$. For $\Delta H_2^{\mathbb{1}}$, $\Delta H_2^{\phi^2}$ we obtain:

$$\Delta H_2^{\mathbb{1}}(\mathcal{E}, E_T) = \frac{s_4 g^2}{2^4 L^2} \sum_{k_1 k_2 k_3 k_4} \frac{1}{\omega_{k_1} \omega_{k_2} \omega_{k_3} \omega_{k_4}} F_0(k_1, k_2, k_3, k_4, \mathcal{E}, E_T), \qquad (5.4)$$

$$\Delta H_2^{\phi^2}(\mathcal{E}, E_T) = \frac{s_3 g^2}{2^4 L^2} \sum_{k_1, k_2, k_3} \sum_{q_1, q_2} \frac{1}{\omega_{k_1} \omega_{k_2} \omega_{k_3}} \frac{1}{\sqrt{\omega_{q_1} \omega_{q_2}}} F_2(k_1, k_2, k_3, q_1, q_2, \mathcal{E}, E_T), \qquad (5.5)$$

where $F_0(k_1, k_2, k_3, k_4, \mathcal{E}, E_T)$ is given by

$$F_{0\,rs} = \delta_{\Sigma_{i=1}^4 k_i, 0} \frac{\theta(\omega_{k_1} + \omega_{k_2} + \omega_{k_3} + \omega_{k_4} + E_{rs} - E_T)}{\mathcal{E} - \omega_{k_1} - \omega_{k_2} - \omega_{k_3} - \omega_{k_4} - E_{rs}} \mathbb{1}_{rs}, \qquad (5.6)$$

and the operator $F_2(k_1, k_2, k_3, q_1, q_2, \mathcal{E}, E_T)$ is given by

$$
\begin{aligned}
F_{2\,rs} = {} & \delta_{k_1+k_2+k_3,q_1}\,\delta_{q_1,-q_2}\,\frac{\theta(E_{rs}+\omega_{k_1}+\omega_{k_2}+\omega_{k_3}-E_T)}{\mathcal{E}-E_{rs}-\omega_{k_1}-\omega_{k_2}-\omega_{k_3}}\,(a_{q_1}a_{q_2})_{rs} \\
& + \delta_{k_1+k_2+k_3,q_1}\,\delta_{q_1,-q_2}\,\frac{\theta(E_{rs}+\omega_{k_1}+\omega_{k_2}+\omega_{k_3}-E_T)}{\mathcal{E}-E_{rs}-\omega_{k_1}-\omega_{k_2}-\omega_{k_3}}\,(a^\dagger_{q_1}a^\dagger_{q_2})_{rs} \\
& + \delta_{k_1+k_2+k_3,q_2}\,\delta_{q_1,q_2}\,\frac{\theta(E_{rs}+\omega_{k_1}+\omega_{k_2}+\omega_{k_3}+\omega_q-E_T)}{\mathcal{E}-E_{rs}-\omega_{k_1}-\omega_{k_2}-\omega_{k_3}-\omega_q}\,(a^\dagger_{q_1}a_{q_2})_{rs} \\
& + \delta_{k_1+k_2+k_3,q_2}\,\delta_{q_1,q_2}\,\frac{\theta(E_{rs}+\omega_{k_1}+\omega_{k_2}+\omega_{k_3}-\omega_q-E_T)}{\mathcal{E}-E_{rs}-\omega_{k_1}-\omega_{k_2}-\omega_{k_3}+\omega_q}\,(a^\dagger_{q_1}a_{q_2})_{rs}\,. \tag{5.7}
\end{aligned}
$$

In eqs. (5.4)–(5.5), all q_i's are bounded from above ($q_i \leq q_{\max}$) because they correspond to the momenta of creation/annihilation operators that act on the light states (i.e. states in $\mathcal{H}_l$). Instead the $k_i = 2\pi n_i/L$ run over all possible values $n_i \in \mathbb{Z}$. Similar expressions for $\Delta H_2^{\phi^4}$, $\Delta H_2^{\phi^6}$, $\Delta H_2^{\phi^8}$ are given in appendix C. As mentioned before, a simple way to derive these expressions from diagrams is given in appendix A. We have performed the same kind of numerical checks done in section 4.3 for all the operators $\Delta\widehat{H}_2$ in the ϕ^4 theory.

Approximations. The exact expressions for ΔH_2 are computationally demanding. Here we present different approximations that speed up the calculations and simplify their analytic structure. These basically consist in approximating the contribution from the highest energy states to ΔH in terms of a local expansion (as normally done in Effective Field Theory calculations), while keeping the contributions from lower energy states in their original non-local form. This is achieved by defining an energy E_L and then by separating ΔH_2 into two parts, ΔH_{2+} where we only sum over intermediate states with $E_j \geq E_L$ and ΔH_{2-} where we sum over those with $E_T < E_j < E_L$.

$$
\Delta H_{2+}(\mathcal{E}, E_L)_{rs} = \Delta H_2(\mathcal{E}, E_L)_{rs}\,, \tag{5.8}
$$

$$
\Delta H_{2-}(\mathcal{E}, E_T, E_L)_{rs} = \Delta H_2(\mathcal{E}, E_T)_{rs} - \Delta H_2(\mathcal{E}, E_L)_{rs}\,. \tag{5.9}
$$

We choose $E_L \gg E_T$ so that ΔH_{2+} is well approximated by local operators.[8] As an example we show how to implement this procedure for the contribution of $\Delta H_2^{\phi^2}$ given in eq. (5.5) and eq. (5.7). We start by examining the term $\Delta H_{2+}^{\phi^2}(\mathcal{E}, E_L) = \Delta H_2^{\phi^2}(\mathcal{E}, E_L)$, which is obtained by replacing E_T by E_L in eq. (5.7). In this case $\sum_i \omega_{k_i} \gtrsim E_L \gg E_T \gtrsim \omega_q, E_{rs}$, and then it can be well approximated by

$$
\Delta H_{2+}^{\phi^2} \simeq c_2\, V_2 \tag{5.10}
$$

with

$$
c_2(\mathcal{E}, E_L) = \frac{s_3 g^2}{(2L)^3} \sum_{k_1, k_2, k_3} \frac{L\,\delta_{k_1+k_2+k_3,0}}{\omega_{k_1}\omega_{k_2}\omega_{k_3}} \frac{\theta(\omega_{k_1}+\omega_{k_2}+\omega_{k_3}-E_L)}{\mathcal{E}-\omega_{k_1}-\omega_{k_2}-\omega_{k_3}}\,, \tag{5.11}
$$

and $V_2 = \int_0^L dx\,\phi^2(x)$ which has dimensions of $[E]^{-1}$. The approximation in eq. (5.10) receives corrections of at most $\mathcal{O}(E_T/E_L)$. The expansion of $\Delta H_{2+}^{\phi^2}$ in terms of local

---

[8]In the cases where we are only interested in having a good approximation for the lower energy entries r, s of the matrix, then E_L can be taken to be similar to E_T.

operators can be obtained by expanding the term $\Delta\widehat{H}_2^{\phi^2}$ in eq. (5.3) around $t, z = 0$

$$\Delta\widehat{H}_2^{\phi^2}(\mathcal{E})_{rs} = -ig^2 s_2 \int_0^\infty dt\, e^{i(\mathcal{E}-E_{rs}+i\epsilon)t} \int_{-L/2}^{L/2} dz D_F^2(z,t) \int_{-L/2}^{L/2} dx \left[:\phi^2(x,0):_{rs} + \mathcal{O}(t^2, z^2) \right], \tag{5.12}$$

and, after integrating, keeping only the contributions from those states that produce poles at $\mathcal{E} > E_L$, when E_{rs} is neglected. On the other hand $\Delta H_{2-}^{\phi^2}(\mathcal{E}, E_T, E_L) = \Delta H_2^{\phi^2}(\mathcal{E}, E_T) - \Delta H_2^{\phi^2}(\mathcal{E}, E_L)$ is given by the same expressions as in eq. (5.5) and eq. (5.7) but now the sums to perform are much smaller since the momenta of the intermediate states are restricted between E_T and E_L.

The same exercise done for $\Delta H_{2+}^{\phi^2}$ can be done for $\Delta H_{2+}^{\mathbb{1}}$ and $\Delta H_{2+}^{\phi^4}$ and one has that in the limit $E_L \gg E_T$

$$\Delta H_{2+}^{\mathbb{1}} \simeq c_0\,\mathbb{1}, \qquad \Delta H_{2+}^{\phi^2} \simeq c_2\,V_2, \qquad \Delta H_{2+}^{\phi^4} \simeq c_4\,V_4, \tag{5.13}$$

where $V_\alpha = \int_0^L dx\, \phi^\alpha(x)$ and has dimensions of $[E]^{-1}$,

$$c_0(\mathcal{E}, E_L) = \frac{s_4 g^2}{(2L)^4} \sum_{k_1,k_2,k_3,k_4} \frac{L\,\delta_{k_1+k_2+k_3+k_4,0}}{\omega_{k_1}\omega_{k_2}\omega_{k_3}\omega_{k_4}} \frac{\theta(\omega_{k_1}+\omega_{k_2}+\omega_{k_3}+\omega_{k_4}-E_L)}{\mathcal{E}-\omega_{k_1}-\omega_{k_2}-\omega_{k_3}-\omega_{k_4}}, \tag{5.14}$$

$$c_4(\mathcal{E}, E_L) = \frac{s_2 g^2}{(2L)^2} \sum_{k_1,k_2} \frac{L\,\delta_{k_1+k_2,0}}{\omega_{k_1}\omega_{k_2}} \frac{\theta(\omega_{k_1}+\omega_{k_2}-E_L)}{\mathcal{E}-\omega_{k_1}-\omega_{k_2}}, \tag{5.15}$$

and c_2 is given in eq. (5.11). On the other hand the operators $\Delta H_2^{\phi^6}$ and $\Delta H_2^{\phi^8}$ are of the tree-level and disconnected type because they involve one and zero propagators respectively, see eq. (5.3). Therefore the operators $\Delta H_{2+}^{\phi^6}$ and $\Delta H_{2+}^{\phi^8}$ are not well approximated by a local expansion, and we do not approximate them. For E_L sufficiently big though, $\Delta H_{2+}^{\phi^6} = \Delta H_{2+}^{\phi^8} = 0$ and all the contribution to $\Delta H_2^{\phi^6}$, $\Delta H_2^{\phi^8}$ comes from $\Delta H_{2-}^{\phi^6}$, $\Delta H_{2-}^{\phi^8}$, as can be explicitly seen from eqs. (C.4)–(C.5). Notice that these operators only contribute to the entries of ΔH_{rs} with high values for E_r, E_s. Again, the coefficients of the local operators in eq. (5.13) can be obtained by expanding $\Delta\widehat{H}_2$ in eq. (5.3) around $t, z = 0$

$$\Delta\widehat{H}_2(\mathcal{E})_{rs} = -ig^2 \int_0^\infty dt\, e^{i(\mathcal{E}-E_{rs}+i\epsilon)t} \int_{-L/2}^{L/2} dx dz \sum_{m=0}^4 s_{4-m} D_F^{4-m}(z,t) :\phi^{2m}(x,0):_{rs} + \mathcal{O}(t,z)^2, \tag{5.16}$$

and, after integrating, keeping only the contributions from those states that produce poles at $\mathcal{E} > E_L$, when E_{rs} is neglected. The evaluation of the coefficients in eq. (5.13) can still be hard to evaluate numerically. In the next section we explain an alternative and simpler derivation of the coefficients c_{2m} and further approximations to evaluate them.

5.2 Local expansion and the phase-space functions

From the first term in the local expansion of eq. (5.16) the coefficients of the local operators are given by:

$$\hat{c}_{2n}(\mathcal{E}) = -ig^2 s_{4-n} \int_0^\infty dt\, e^{i(\mathcal{E}+i\epsilon)t} \int_{-\infty}^\infty dx\, D_F^{4-n}(x,t), \tag{5.17}$$

where s_{4-n} is the symmetry factor and, as explained above, the common E_{rs}-shift on the eigenvalue $\mathcal{E}$ is neglected.[9] Next, applying the Kramers-Kronig dispersion relation to $c_n(\mathcal{E})$ in eq. (5.17)

$$\hat{c}_{2n}(\mathcal{E}) = -\int_{-\infty}^{\infty} \frac{dE}{\pi} \frac{1}{\mathcal{E} - E + i\epsilon} \operatorname{Im} \hat{c}_{2n}(\mathcal{E}) \,. \tag{5.18}$$

Next, we compute $\operatorname{Im} \hat{c}_{2n}$. First we do the space integral which, up to $g^2 s_{4-n}$, yields

$$\operatorname{Im} -i \sum_{k's} \frac{L\,\delta_{\sum_i k_i, 0}}{\prod_i 2L\omega_{k_i}} \int_0^{\infty} dt\, e^{i(E-\sum_i \omega_{k_i}+i\epsilon)t} = -\frac{1}{2} \sum_{k's} \frac{L\,\delta_{\sum_i k_i, 0}}{\prod_i 2L\omega_{k_i}} 2\pi\delta\left(E - \sum_i \omega_{k_i}\right), \tag{5.19}$$

where we have used $D_F(t,x)\theta(t) = D(t,x)\theta(t)$ with $D(t,x) = \sum_k (2L\omega_k)^{-1} e^{ikx - i\omega_k t}$. Therefore we find,[10]

$$\hat{c}_{2n}(\mathcal{E}) = \frac{g^2 s_{4-n}}{2\pi} \int_{-\infty}^{\infty} \frac{dE}{\mathcal{E} - E + i\epsilon} \Phi_{4-n}(E) \tag{5.20}$$

where $\Phi_m(E)$ is the m-particle phase space

$$\Phi_m(E) = \sum_{k_1, k_2, \ldots, k_m} \frac{L\,\delta_{\sum_{i=1}^m k_i, 0}}{\prod_{i=1}^m 2L\omega_{k_i}} 2\pi\delta\left(E - \sum_{i=1}^m \omega_{k_i}\right). \tag{5.21}$$

Finally, the coefficients in eq. (5.13) are obtained by including only the contributions from poles located at $\mathcal{E} \geq E_L$

$$c_0(\mathcal{E}) = s_4\, g^2 \int_{E_L}^{\infty} \frac{dE}{2\pi} \frac{1}{\mathcal{E} - E} \Phi_4(E) \,, \tag{5.22}$$

$$c_2(\mathcal{E}) = s_3\, g^2 \int_{E_L}^{\infty} \frac{dE}{2\pi} \frac{1}{\mathcal{E} - E} \Phi_3(E) \,, \tag{5.23}$$

$$c_4(\mathcal{E}) = s_2\, g^2 \int_{E_L}^{\infty} \frac{dE}{2\pi} \frac{1}{\mathcal{E} - E} \Phi_2(E) \,. \tag{5.24}$$

It would be interesting to see if in general, higher ΔH_{n+} corrections can also be written in terms of phase space functions. In the rest of the section we explain useful approximations to evaluate eqs. (5.22)–(5.24).

Continuum and high energy limit of the phase space. We start by approximating the phase space by its continuum limit.[11] Recall that in the continuum limit the relativistic phase-space for n-particles is given by

$$\Phi_n(E) = \int \prod_{i=1}^{n} \frac{dk_i^1}{(2\pi)\, 2\omega_{k_i}} (2\pi)^2 \delta^{(2)}\left(P^\mu + \sum_{i=1}^{n} k_i^\mu\right), \tag{5.25}$$

where $P^\mu = (E, 0)$ and $k_i^\mu = (\omega_{k_i}, k_i)$. Then, for the 2-body phase space one has

$$\Phi_2(E) = \frac{1}{E\sqrt{E^2 - 4m^2}} \,. \tag{5.26}$$

---

[9]The derivation of the coefficients $\hat{c}_{2n}(\mathcal{E})$ in eq. (5.17) applies to any ϕ^α theory.

[10]Eq. (5.20) can also be derived from the optical theorem, with careful treatment of the symmetry factors.

[11]This is a good approximation for $Lm \gg 1$ and we have checked it explicitly in our numerical study.

Next, solving for the Dirac delta's in eq. (5.25), the 3-body phase-space is given by

$$\Phi_3(E) = \frac{1}{2\pi} \int_{4m^2}^{(E-m)^2} \frac{ds_{23}}{\sqrt{s_{23}\big(s_{23} - [E+m]^2\big)\big(s_{23} - [E-m]^2\big)\big(s_{23} - 4m^2\big)}}\,, \qquad (5.27)$$

with $E \geq 3m$. This integral can be solved by standard Elliptic integral transformations and we obtain,

$$\Phi_3(E) = \frac{g^2}{\pi} \frac{1}{(E-m)} \frac{1}{\sqrt{(E+m)^2 - 4m^2}} K(\alpha)\,, \qquad (5.28)$$

where $\alpha = 1 - \frac{16Em^3}{(E-m)^3(E+3m)}$ and $K(\alpha) = \int_0^{\pi/2} \frac{d\varphi}{\sqrt{1-\alpha\sin^2(\varphi)}}$ is an elliptic integral.

In general though, finding the exact phase space functions $\Phi_n(E)$ is difficult but can be simplified in the limit $E \gg m$. In our case, this limit is justified because the phase space functions are evaluated for $E \geq E_L \gg m$. Notice that to take the high energy limit of $\Phi_n(E)$ one can not expand the integrand of eq. (5.25) because, after solving for the Dirac delta's constraints, it is of $\mathcal{O}(1)$ at the integral limits, see for instance the elliptic integral in eq. (5.27). Instead, we use the following relation for the phase space

$$I_n(\tau) \equiv \int_{-\infty}^{\infty} dx\, D_E^n(x,\tau) = \frac{1}{2\pi} \int_0^{\infty} dE\, e^{-E\tau} \Phi_n(E) \qquad (5.29)$$

where $D_E(x,\tau)$ is the euclidean propagator and $\Phi_n(E)$ is only non vanishing for $E \geq n\,m$. The Euclidean propagator in $d = 2$ is given by the special Bessel function of second kind $K_0(m\rho)$ with $\rho = \sqrt{x^2 + \tau^2}$ and $I_n(\tau) \equiv \int_{-\infty}^{\infty} dx\, K_0^n(m\rho)(2\pi)^{-n}$. At this point we can use a clever trick done in ref. [1] to find the leading terms of the inverse Laplace transform of $I_n(\tau)$ in the limit $E \to \infty$. Since the phase space $\Phi_n(E)$ is the inverse Laplace transform of $I_n(\tau)$, the leading parts of $\Phi_n(E)$ as $E \to \infty$ come from the non-analytic parts of $I_n(\tau)$ as $\tau \to 0$. To find the non-analytics parts of $I_n(\tau)$ first one notices that

$$K_0(m\rho) = \begin{cases} -\log\big(\frac{e^\gamma m\rho}{2}\big)\big[1 + \mathcal{O}(m^2\rho^2)\big]\,, & \rho \ll 1/m \\ \sqrt{\frac{\pi}{2m\rho}}\, e^{-m\rho}\big[1 + \mathcal{O}(m^{-1}\rho^{-1})\big]\,, & \rho \gg 1/m \end{cases} \qquad (5.30)$$

where γ is the Euler constant. Then, the contributions to $I_n(\tau) = \int_{-\infty}^{\infty} dx\, K_0^n(m\rho)(2\pi)^{-n}$ when $\tau \to 0$ are dominated by the region where $\rho \ll 1/m$ and the integrand can be approximated by $K_0(m\rho) \approx -\log\big(\frac{e^\gamma m\rho}{2}\big)$.[12] This approximation introduces spurious IR divergences in the region of integration $\rho \gg 1/m$ where the approximation of the integrand is not valid. These divergences can be regulated with a cutoff Λ or, equivalently, one can take derivatives with respect to the external coordinate τ to regulate the integral $I_n(\tau)$.[13] Hence, approximating $K_0(m\rho) \approx -\log\big(\frac{e^\gamma m\rho}{2}\big)$ and integrating over x one can find the non-analytic terms of $\partial_\tau I_n(\tau)$ as $\tau \to 0$. For instance, for $n = 4$

$$\partial_\tau I_4(\tau) = \frac{1}{4\pi^3} \log(m\tau e^\gamma)\left[\log(m\tau)\log(m\tau e^{2\gamma}) + \gamma^2 + \frac{\pi^2}{4}\right] + \text{const.} + \mathcal{O}(\tau)\,, \qquad (5.31)$$

---

[12]This method is like the method of regions which is used to get the leading terms of multi-loop Feynman diagrams in certain kinematical limits or mass hierarchies.

[13]This is similar to the fact that the UV divergences of multi-loop Feynman diagrams are polynomial in the external momenta because taking enough derivatives with respect to the external momenta the integrals are UV finite.

where the constant does not depend on τ. Lastly from eq. (5.29), $\partial_\tau I_n(\tau)$ is related to the phase space $\Phi_n(E)$ by the Laplace transform,

$$\int_0^\infty dE[-E\Phi_n(E)]\,e^{-\tau E} = 2\pi\,\partial_\tau I_n(\tau) \tag{5.32}$$

so that for $n = 4$ one has

$$\Phi_4(E) = \frac{3}{2\pi^2}\frac{1}{E^2}\big[\log^2(E/m) - \pi^2/12\big] + \mathcal{O}(m^2/E^4)\,. \tag{5.33}$$

Therefore using eq. (5.33) and expanding eqs. (5.26), (5.28) at large E,

$$c_0(\mathcal{E}) \simeq s_4\,g^2 \int_{E_L}^\infty \frac{dE}{2\pi}\frac{1}{\mathcal{E}-E}\frac{3}{2\pi^2}\frac{1}{E^2}\big[\log^2(E/m) - \pi^2/12\big]\,, \tag{5.34}$$

$$c_2(\mathcal{E}) \simeq s_3\,g^2 \int_{E_L}^\infty \frac{dE}{2\pi}\frac{1}{\mathcal{E}-E}\frac{3}{2\pi}\frac{1}{E^2}\log(E/m)\,, \tag{5.35}$$

$$c_4(\mathcal{E}) \simeq s_2\,g^2 \int_{E_L}^\infty \frac{dE}{2\pi}\frac{1}{\mathcal{E}-E}\frac{1}{E^2}\,, \tag{5.36}$$

where the error made in the approximations is of the order $\mathcal{O}(m^2/E_L^2)$. We end this section by noticing that the leading terms of the phase space functions $\Phi_2(E)$ and $\Phi_3(E)$ in the large E expansion agree with the corresponding result of ref. [1] (there called $\mu_{444}(E) = s_2\Phi_2(E)/(2\pi)$, $\mu_{442}(E) = s_3\Phi_3(E)/(2\pi)$). The local approximation in eqs. (5.34)–(5.36) can be refined by taking into account the E_{rs} shift, see ref. [1].

5.3 Spectrum and convergence

Before starting with the numerical results we first discuss the series $\Delta H = \sum_{n=2}\Delta H_n$ in more detail. The truncation of the ΔH series in powers of $(V_{hh}/H_{0\,hh})^n$ is only justified for $V_{hh}/H_{0\,hh} < 1$. Notice that even for weak coupling $g \ll 1$ the series does not seem to converge. Let us consider a particular matrix entry

$$\langle E_r\,|\Delta H_n|\,E_s\,\rangle = \sum_{j_1,\dots,j_{n-1}} V_{rj_1}\cdots V_{j_{i-1}j_i}\frac{1}{\mathcal{E}-E_{j_i}}\cdots\frac{1}{\mathcal{E}-E_{j_{n-1}}}V_{j_{n-1}s}\,, \tag{5.37}$$

where all the terms in the sums have a definite sign depending on whether n is even or odd. For instance, consider a contribution to eq. (5.37) from states of high occupation number but low momentum like

$$V_{j_{i-1}j_i}\frac{1}{\mathcal{E}-E_{j_i}} \rightarrow \frac{\langle N_kN_{-k}\,|V|\,N_kN_{-k}\,\rangle}{\mathcal{E}-2N\omega_k} = \frac{6g}{4L\omega_k^2}\frac{(2N(N-1)+4N^2)}{\mathcal{E}-2N\omega_k}\,, \tag{5.38}$$

where $|\,N_kN_{-k}\,\rangle$ is a Fock state with N particles of momentum k and $-k$ that satisfy $2N\omega_k > E_T$. The term of eq. (5.38) gives a non-perturbative contribution even for small g for high enough N and becomes worse for smaller momentum $|k|$. Thus the series $(\Delta H)_{rs} = \sum(\Delta H_n)_{rs}$ seems to be non-convergent but we will assume that (when the expansion parameter is small) the first terms of the series are a good approximation to $(\Delta H)_{rs}$. Notice that the appearance of the non-perturbative contributions (like in eq. (5.38)) can

be worse for those matrix entries $(\Delta H)_{rs}$ with energies $E_{r,s}$ closer to E_T because the intermediate states in $V_{jj'}$ can have lower momentum and high occupation number for a given ΔH_n.

For the first terms of the expansion $(V_{hh}/E_h)^n$, a naive estimate of the dimensionless expansion parameter is $\alpha_{rs} \sim g/E_T \times 1/(L\mu_{rs}^2)$ where the g and L can be read off from the potential; the E_T^{-1} arises because the sums in eq. (5.37) are dominated by the first terms, starting at $1/E_T$ (for $\mathcal{E} \ll E_T$); and by direct inspection of the potential $m/N \lesssim \mu_{rs} \lesssim E_T$ where N is a possibly large occupation number, depending on the matrix entry.

It can happen that entries with energies E_r, E_s close to E_T do not have a perturbative $(\Delta H)_{rs} = \sum (\Delta H_n)_{rs}$ expansion and even including the first terms of the series is a worse approximation than setting $(\Delta H)_{rs} \to 0$; these entries can induce big errors on the computed eigenvalues. Since the eigenvalues we are interested in computing are mostly affected by the lower $E_{r,s}$-energy matrix entries we will neglect the renormalization of the higher $E_{r,s}$ energy entries where the series $(\Delta H)_{rs} = \sum (\Delta H_n)_{rs}$ is not perturbative. One way to select those entries would be to keep only those that satisfy $\alpha_{rs} \sim (\Delta H_3)_{rs}/(\Delta H_2)_{rs} < 1$. However, this can be computationally expensive and instead we take a more pragmatic approach and only renormalize those matrix entries $(H_T)_{rs}$ with either E_r or E_s below some conservative cutoff E_W, below which the series is perturbative.

Up until this point the discussion has been done for $g \ll 1$. However, for those matrix entries where α_{rs} is a perturbative expansion parameter one can increase g to strong coupling[14] by increasing E_T at the same time. Increasing E_T means enlarging the size of H_T and ΔH, and it can happen that the new matrix entries do not have a perturbative $(\Delta H)_{rs} = \sum (\Delta H_n)_{rs}$ expansion. As explained above, in those cases we set $(\Delta H)_{rs}$ to zero.[15]

Numerical results. In the rest of the section we perform a numerical study of the spectrum of the ϕ^4 theory. First we summarize the concrete implementation of the method. We find the spectrum of H by diagonalizing $H_{\text{eff}} = H_T + \Delta H_2(\mathcal{E}^T)$ where $\mathcal{E}^T$ is the eigenvalue of H_T.[16] As explained in section 5.1, to calculate ΔH_2 we separate it in ΔH_{2+} and ΔH_{2-} defined in eqs. (5.8)–(5.9) and take $E_L = 3E_T$.[17] We found little differences when iterating the diagonalization with $\mathcal{E}$. We also find that increasing E_L does not have a significant effect on the result. For $\Delta H_{2-}(\mathcal{E}, E_T, E_L)$ we use the expressions in eqs. (C.1)–(C.5) and for $\Delta H_{2+}(\mathcal{E}, E_L)$ we use the ones in eqs. (5.34)–(5.36). We do a conservative estimate of the expansion parameter α_{rs} and set to zero $(\Delta H_2)_{rs}$ for all those entries that are not perturbative.

First we study the lowest eigenvalues of H at weak coupling, where we can compare with standard perturbation theory. The perturbative corrections to the vacuum and the

---

[14]In the ϕ^4 theory the strong coupling can be estimated to be $g \gtrsim 1$, see eqs. (5.39) and (5.40).

[15]For the ϕ^2 perturbation studied in section 4 we find that the error in the computed eigenvalues can be decreased by increasing E_T even without introducing E_W. For the ϕ^4 we find that E_W must be introduced.

[16]The dimension of the Hilbert space $\mathcal{H}_{ll}$ for $E_T = 10, 12, 14, 16$ and 18 is $117(108), 309(305), 827(816), 2160(2084)$ and $5376(5238)$ for the $\mathbb{Z}_2$-even(odd) sectors, respectively.

[17]The choice $E_L = 3E_T$ is done so that the local expansion is a good approximation for intermediate states with $E_j \geq E_L$. Also, for this E_L one has that $\Delta H_{2+}^{\phi^6} = \Delta H_{2+}^{\phi^8} = 0$.
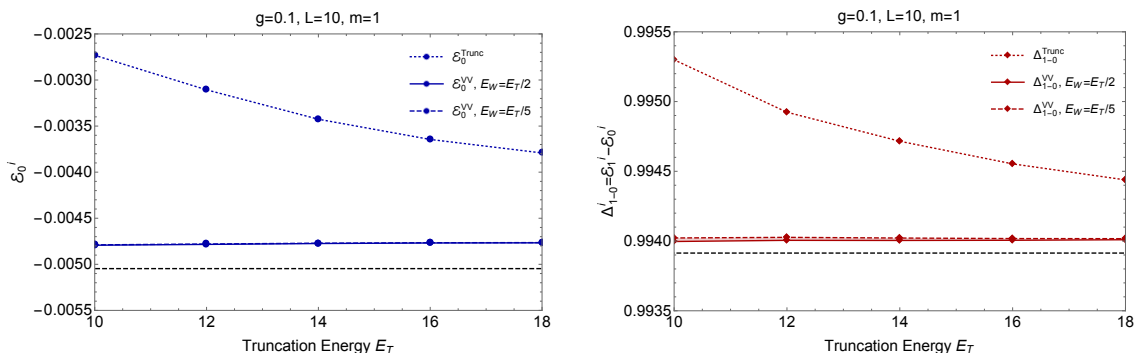
Figure 5. *Left*: the vacuum energy $\mathcal{E}_0^i$ as a function of the truncation energy E_T for a coupling of $g = 0.1$. *Right*: energy difference between the first $\mathbb{Z}_2$-odd excited state and the vacuum energy $\mathcal{E}_0^i$ as a function of the truncation energy for $g = 0.1$. In both plots, the dotted curves are computed with the truncated Hamiltonian while the solid and dashed curves are computed with the renormalized hamiltonian at order VV. Dashed and dotted lines correspond to the cutoffs $E_W = E_T/2$ and $E_W = E_T/5$. We have overlaid two dashed black lines corresponding to the calculation in perturbation theory, see eqs. (5.39) and (5.40).

mass are given by [1]:

$$\Lambda/m^2 = -\frac{21\xi(3)}{16\pi^3}\,\bar{g}^2 + 0.04164(85)\,\bar{g}^3 + \dots, \tag{5.39}$$

$$m_{\mathrm{ph}}^2 = m^2\left[1 - \frac{3}{2}\bar{g}^2 + 2.86460(20)\,\bar{g}^3 + \cdots\right], \tag{5.40}$$

where $\bar{g} \equiv g/m$ and m_{ph} is the physical mass. In figure 5 we show the result for the vacuum energy and m_{ph}. As explained before, only those entries with $E_{r,s}$ energies below a cutoff E_W are renormalized. We do the plot for different values of $E_W = E_T/2, E_T/5$ and we find that the vacuum energy and the physical mass do not depend much on this cutoff. For the left plot the difference between $E_W = E_T/2$ and $E_W = E_T/5$ is inappreciable.[18] We find that the spectrum is much flatter as a function of E_T for renormalized eigenvalues than the ones computed with H_T. Since the exact spectrum is independent of the truncation energy E_T, a flatter curve in E_T indicates a closer value to exact energy levels. However, it could still happen that adding ΔH_3 corrections shifted the spectrum by a small amount, as it happens for the ϕ^2 perturbation seen in figures 3 and 4 for the range $16 \lesssim E_T \leq 20$. In the plots we have superimposed constant dashed black lines that are obtained from the perturbative calculations in eq. (5.39) and eq. (5.40). We find that the eigenvalues computed with ΔH_2 are much closer to the perturbative calculation than the ones done with H_T. The difference between the perturbative result and the one from $\mathcal{E}^{VV}$ is of $\mathcal{O}(10^{-4})$ and can be attributed to higher order corrections in the perturbative expansion. Another source of uncertainty comes from higher order ΔH_n corrections not included.

---

[18]In fact, for this case we have checked that setting $E_W = E_T$ gives a result on top of the lines of $E_W = E_T/2$. This is because at weak coupling there is not much overlap between the lowest lying eigenstates of H and the high H_0 eigenstates.
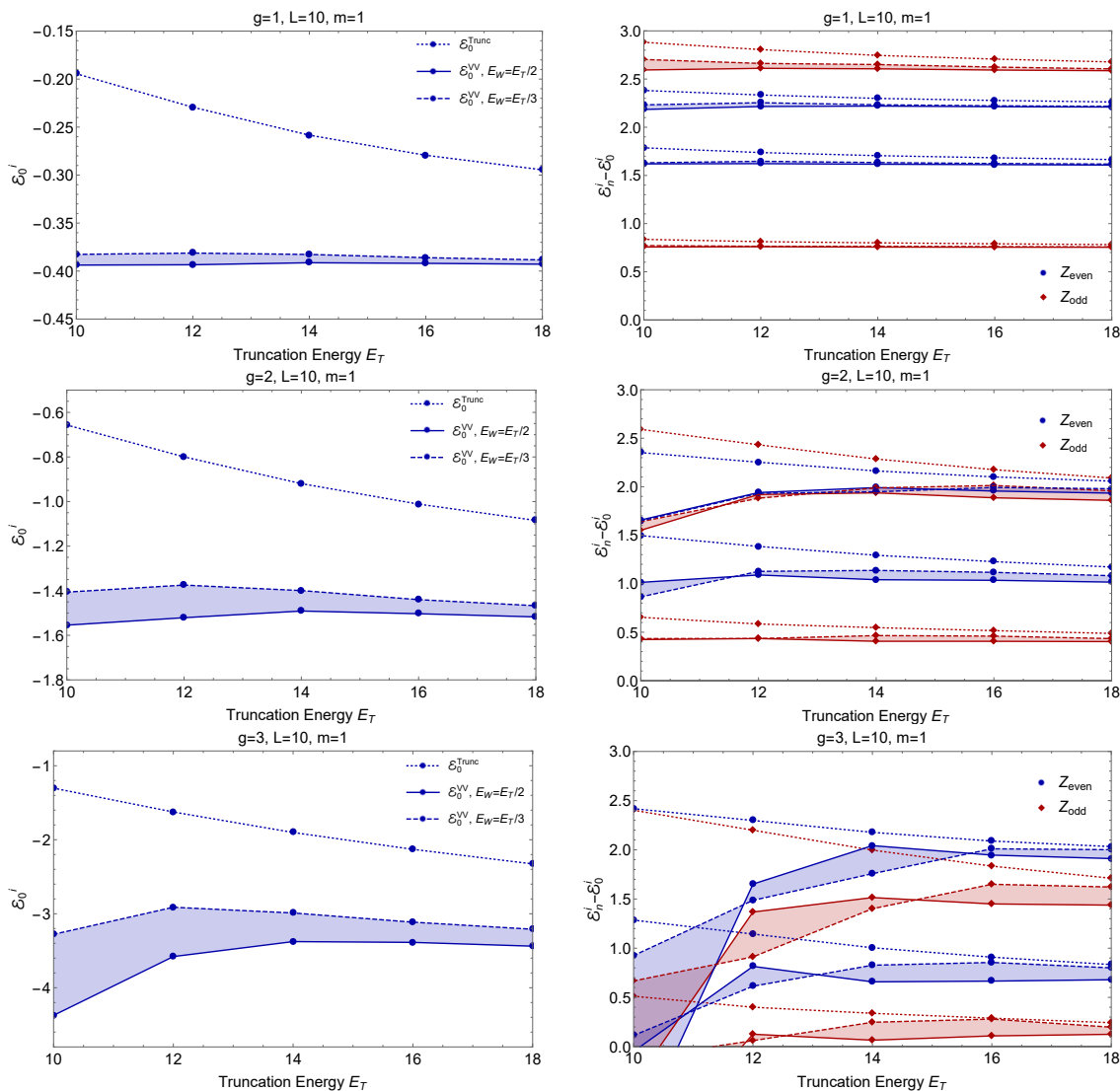
Figure 6. *Left*: the vacuum energy $\mathcal{E}_0^i$ as a function of E_T for $g = 1$, 2 and 3 in descending order. *Right*: energy difference between the first excited states and the vacuum energy as a function of the coupling E_T for $g = 1$, 2 and 3. In all the plots of the figure the blue curves correspond to the $\mathbb{Z}_2$-even sector while the red ones to the $\mathbb{Z}_2$-odd. The dotted curves are computed with the truncated Hamiltonian, while the solid and dashed lines are computed adding ΔH_2 with cutoffs $E_W = E_T/2$ and $E_W = E_T/3$.

In figure 6 we show plots with different energy levels as a function of the truncation energy E_T for $g = 1$, 2, 3. To compare with previous work, these plots have been done with the same choice of parameters and normalizations as in figures 9–10 of ref. [1]. In all the plots the dotted lines are computed using the truncated Hamiltonian while the solid and dashed lines are computed using ΔH_2 with $E_W = E_T/2$ and $E_W = E_T/3$, respectively. The diamonds and the circles correspond to states in the $\mathbb{Z}_2$-even and $\mathbb{Z}_2$-odd sectors of the theory. We find that in all the plots, for high enough values of E_T, the solid lines
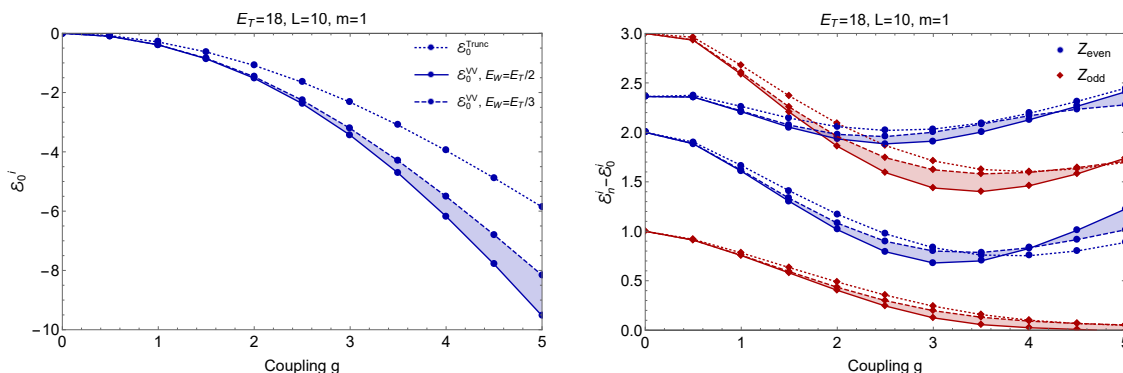
Figure 7. *Left*: the vacuum energy $\mathcal{E}_0$ as a function of the coupling g. *Right*: energy difference between the first excited states and the vacuum energy as a function of the coupling constant g. In all the plots of the figure the blue curves correspond to the $\mathbb{Z}_2$-even sector while the red ones to the $\mathbb{Z}_2$-odd. The dotted curves are computed with the truncated Hamiltonian for a truncation energy $E_T = 18$, while the solid and dashed lines are computed adding ΔH_2 with cutoffs $E_W = E_T/2$ and $E_W = E_T/3$.

for the ΔH_2 are flatter than the truncated ones. The difference between the dotted and dashed lines is bigger for the plot for $g = 3$ than the one for $g = 1$. This can be understood because one expects more overlap from higher H_0 excited states with the vacuum for higher coupling. The difference between the solid and dashed lines becomes smaller as E_T is increased. This can be understood because as E_T is increased bigger parts of $(H_T)_{rs}$ are being renormalized, and eventually the difference between using $E_W = E_T/2$ and $E_T/3$ becomes negligible. An intrinsic error of our calculation of the eigenvalues is the difference between the values obtained for different choices of E_W. This error could be reduced with a more careful estimate of the expansion parameter $\alpha_{r,s}$, which would be very interesting for the future development of the method. In fact, it seems that for $E_T \lesssim 12(14)$ for $g = 2(3)$ the cutoff E_W is too high (and might include non-perturbative corrections like the one in eq. (5.38)) as the eigenvalues deviate a lot from the computation done with H_T. Another small source of uncertainty in our calculation comes from not having included higher order ΔH_n corrections; in the next section we explain the calculation of ΔH_3.

In figure 7 we show two plots of the vacuum and first excited states as a function of the coupling constant g for $E_T = 18$ (cf. figure 4 of ref. [1]). There is an intrinsic uncertainty in our procedure in the choice of E_W, and as we discussed above it could be lowered by increasing the size of the truncation E_T or ideally by refining the determination of E_W. Notice that the renormalization of the truncated Hamiltonian matters as the solid lines have a significant difference with respect to the truncated (as seen in figure 6 the solid lines show a better convergence as a function of E_T). For $g \gtrsim 3.5$ the first $\mathbb{Z}_2$-odd excited state seems to become degenerate with the vacuum which is a signal of the spontaneous breaking of the $\mathbb{Z}_2$ symmetry. This plot can be used to determine the critical coupling, see ref. [1].

5.4 Three point correction and further comments

As explained in the previous section we have performed the numerical study of the ϕ^4 theory without taking into account the three point correction ΔH_3. This would be an interesting point for the future and therefore we give a small preview of the type of expressions one obtains when computing the three point correction. As done throughout the paper, to get the expression for ΔH_3 we start by first computing

$$\Delta \widehat{H}_3(\mathcal{E})_{rs} = -\lim_{\epsilon \to 0} \int_0^\infty dt_1 dt_2 \, e^{i(\mathcal{E}-E_r+i\epsilon)(t_1+t_2)} \mathcal{T}\{V(T_1)V(T_2)V(T_3)\}_{rs} , \qquad (5.41)$$

where $T_k = \sum_{n=1}^{3-k} t_n$. Then we find ΔH_3 by keeping only those terms that have all poles at $\mathcal{E} > E_T$. Then, we see that the three point correction can be split into

$$\Delta H_3 = \Delta H_3^{\mathbb{1}} + \Delta H_3^{\phi^2} + \Delta H_3^{\phi^4} + \Delta H_3^{\phi^6} + \Delta H_3^{\phi^8} + \Delta H_3^{\phi^{10}} + \Delta H_3^{\phi^{12}} , \qquad (5.42)$$

where the subindices denote the number of fields in each term. The correction $\Delta H_3^{\mathbb{1}}$ is given by

$$\Delta H_3^{\mathbb{1}}(\mathcal{E}) = \frac{s_{222}\, g^3}{(2L)^6} \sum_{k_i,p_i,l_i} \frac{L^2 \delta_{p_1+p_2+k_1+k_2,0}^{l_1+l_2+k_1+k_2,0}}{\omega_{k_1}\omega_{k_2}\omega_{p_1}\omega_{p_2}\omega_{l_1}\omega_{l_2}} \frac{\theta(\Sigma_{i=1}^2[\omega_{p_i}+\omega_{k_i}]-E_T)}{\mathcal{E}-\Sigma_{i=1}^2[\omega_{p_i}+\omega_{k_i}]} \frac{\theta(\Sigma_{i=1}^2[\omega_{l_i}+\omega_{k_i}]-E_T)}{\mathcal{E}-\Sigma_{i=1}^2[\omega_{l_i}+\omega_{k_i}]} . \qquad (5.43)$$

where the symmetry factor is defined in eq. (4.20). The rest of the terms $\Delta H_3^{\phi^2}, \cdots, \Delta H_3^{\phi^{12}}$ can be computed in a similar fashion as explained in previous sections, but we do not present them here since we did not include them in the numerical analysis.

Another interesting thing to study in the future is the local expansion of ΔH_3 and higher orders in ΔH_n. Here we present some of the terms for the ΔH_3 case. As done for ΔH_2, when the local expansion applies the calculation is simplified. We use the diagrammatic representation explained in appendix A for the expressions at $\mathcal{O}(t^0, z^0)$ of the local renormalization. As an example the leading local coefficients that renormalize the operators V_2, V_4 and V_6 are

$$\Delta H_{3+}^{\phi^2} \simeq \Big(\text{⬡} + \text{⬡} + \text{⬡} + \text{⬡} + \cdots \Big) V_2 \qquad (5.44)$$

where for example,

$$\text{⬡} = \frac{s_{131}\, g^3}{(2L)^5} \sum_{k,l,p_i} \frac{L^2 \delta_{p_1+p_2+p_3+k,0}^{l+k,0}}{\omega_k \omega_{p_1} \omega_{p_2} \omega_{p_3}} \frac{\theta(\omega_l+\omega_k-E_L)}{\mathcal{E}-\omega_l-\omega_k} \frac{\theta(\omega_k+\Sigma_{i=1}^3 \omega_{p_i}-E_L)}{\mathcal{E}-\omega_k-\Sigma_{i=1}^3 p_i} . \qquad (5.45)$$

For the renormalization of the quartic we get

$$\Delta H_{3+}^{\phi^4} \simeq \Big(\text{⬡} + \text{⬡} + \text{⬡} + \cdots \Big) V_4 \qquad (5.46)$$

where for example,

$$\text{⬡} = \frac{s_{220}\, g^3}{(2L)^4} \sum_{l_1 l_2 p_1 p_2} \frac{L^2 \delta_{l_1+l_2,0}^{p_1+p_2,0}}{\omega_{l_1}\omega_{l_2}\omega_{p_1}\omega_{p_2}} \frac{\theta(\omega_{l_1}+\omega_{l_2}-E_L)}{\mathcal{E}-\omega_{l_1}-\omega_{l_2}} \frac{\theta(\omega_{p_1}+\omega_{p_2}-E_L)}{\mathcal{E}-\omega_{p_1}-\omega_{p_2}} . \qquad (5.47)$$

For V_6

$$\Delta H_{3+}^{\phi^6} \simeq \left(\text{} + \cdots \right) V_6 \tag{5.48}$$

where

$$\text{} = \frac{s_{111}\, g^3}{(2L)^3} \sum_k \frac{L^2}{m\, \omega_k^2} \left(\frac{1}{\mathcal{E} - 2\omega_k} \right)^2 \theta(2\omega_k - E_L)\,. \tag{5.49}$$

As final remark, notice that the expression in eq. (5.47) is the square of the coefficient of V_4 (in $\Delta H_{2+}^{\phi^4}$) up to a numerical factor (see eq. (5.15))

$$\left(\text{} \right)^2 = 6g\, \text{}\,. \tag{5.50}$$

It would be very interesting to investigate whether certain classes of diagrams in the $\Delta H_+ = \sum_n \Delta H_{n+}$ expansion can be resumed. This would reduce the error in the computed spectrum and its dependence on the arbitrary truncation energy E_T. For instance, it could be that the resummation comes only from the leading pieces of the different diagrams.[19]

5.5 Summary of the method and comparison with ref. [1]

In this section we summarize our approach to the renormalized Hamiltonian truncation method and briefly comment on the main differences with ref. [1].

The aim of the renormalized Hamiltonian truncation method is to find the lowest eigenvalues $\mathcal{E}$ of H. This is done by diagonalizing $H_{\text{eff}} \equiv H_T + \Delta H$, where H_T is the truncated Hamiltonian and ΔH encodes the contributions from the H_0 eigenstates with $E > E_T$. Computing ΔH is difficult but the problem is simplified if one expands ΔH in powers of V_{hh}/H_{hh}. One expects that the first terms of the series $\Delta H = \sum_n \Delta H_n$ are a good approximation to ΔH if the expansion parameter is small. These terms can be computed as explained in section 2, by first finding $\Delta \widehat{H}_n$ and keeping only the contributions from the states with $E > E_T$. Then, we notice that for some entries with E_r, E_s close to E_T, the series $(\Delta H)_{rs} = \sum_n (\Delta H_n)_{rs}$ is not perturbative (for the chosen parameters g, E_T). We deal with this problem by setting to zero all those entries with E_r or $E_s > E_W$ where E_W is chosen appropriately, see section 5.3.

In order to speed up the numerics and gain analytic insight, we perform several approximations to the exact expression of ΔH_2. First we introduce a scale E_L so that $\Delta H_2 = \Delta H_{2-} + \Delta H_{2+}$ where ΔH_{2+} only receives contributions of the states with $E \geq E_L$ while ΔH_{2-} only receives contributions of states with $E_T < E < E_L$. The scale E_L is chosen such that ΔH_{2+} can be well approximated by the first terms of a local expansion. In our case, we only keep the leading terms $\Delta H_{2+} = \sum_{n=0}^{n=2} c_{2n} \int dx\, \phi^{2n}(x,t)$ and we find that the coefficients c_i can be written in terms of phase space functions. Lastly, the coefficients c_i are approximated by taking the continuum limit and then expanding them in powers of m/E_L. On the other hand ΔH_{2-} is kept exact because its numerical implementation is less costly and it does not admit an approximation by truncating a local expansion. The whole procedure has been described in section 5 and used to do the plots of section 5.3.

---

[19]This is the case in standard perturbation theory. For example the Renormalization Group Equations in $d = 4$ resum the leading logs coming from different diagrams.

Comparison with ref. [1]. Refs. [1, 3] introduced a renormalized Hamiltonian truncation method by diagonalizing $H_{\text{eff}} = H_T + \Delta H$ and expanding ΔH in a series. As explained, we have used this as our starting point. In ref. [1] though an approximation to ΔH_2 is calculated using a different approach than in this paper. To get ΔH_2, ref. [1] starts by defining the following operator $M(E)$

$$M(E)_{rs} \, dE \equiv \sum_{E_j \leq E \leq E_j + dE} V_{rj} V_{js} \quad \text{such that} \quad \Delta H_2 = \int_{E_T}^{\infty} dE \, \frac{M(E)}{\mathcal{E} - E}, \qquad (5.51)$$

and then noticing that $M(E)$ is related to the matrix element

$$C(\tau)_{rs} \equiv \langle r \, | V(\tau/2) \, V(-\tau/2) | \, s \rangle = \int_{0}^{\infty} dE \, e^{-[E - (E_r + E_s)/2]\tau} \, M(E)_{rs} \qquad (5.52)$$

by a Laplace transform. In ref. [1], the $E \to \infty$ behavior of $M(E)$ is found by doing the inverse Laplace transform of the non-analytic parts of $C(\tau)$ in the limit $\tau \to 0$. This is done in the continuum limit, which is a good approximation. The obtained result for $M(E)$ in this limit is taken to compute ΔH_2. Ref. [1] differentiates two renormalization procedures, one where the term $(E_r + E_s)/2$ in eq. (5.52) is approximated to zero (called local), and one where it is taken into account (called sub-leading). In the later case $M(E)$ is given by $M(E - E_{rs})$, and therefore for entries with $E_{rs} \sim E_T$ taking the limit $E - E_{rs} \gg m$ is not justified when $E \sim E_T$. The way in which this problem is dealt with is by neglecting all the contributions of $M(E - E_{rs})$ for $E \leq E_{rs} + 5m$; in other words, a $\theta(E - E_{rs} - 5m)$ is multiplied to the integrand in eq. (5.51).[20]

With this, we can already find the main differences between the two approaches. In our case we calculate the exact expression of ΔH_2 which, if needed, can be approximated. Instead, ref. [1] finds the contributions of ΔH_2 that are leading in the limit where $E \to \infty$ (which neglects the tree and disconnected contributions). From our approach we can recover the local result of ref. [1] if we set $E_L = E_W = E_T$, neglect the tree and disconnected contributions, take the continuum limit, perform a local expansion to ΔH_{2+}, and make an expansion in $m/E \ll 1$. The choice $E_L = E_T$ implies $\Delta H_2 = \Delta H_{2+}$ and $\Delta H_{2-} = 0$, while $E_W = E_T$ means that no entries $(\Delta H_2)_{rs}$ are set to zero. In a similar way we can recover the sub-leading result taking into account the E_{rs} terms, while introducing by hand a $\theta(E - E_{rs} - 5m)$ in the integrals of the coefficients.

Even though the two approaches are quite different, our method and their sub-leading renormalization can still give similar results due to the following. For large enough E_T, the low entries of $(\Delta H_2)_{rs}$ only receive contributions from loop-generated operators,[21] and can be well approximated by a local (up to the E_{rs} dependence) expansion even if $E_L = E_T$. On the other hand, for high energy entries of $(\Delta H_2)_{rs}$ the tree and disconnected operators are non-zero, and none of the operators can be approximated by a truncated local expansion if $E_L = E_T$. However, in many cases these high energy entries become non perturbative and we set them to zero when E_r or $E_s > E_W$. Therefore we find that if E_W is used, it

---

[20]They find that $M(E)$ starts to be well approximated by the first terms in the m/E expansion when $E \geq 5m$.

[21]This can be easily seen from the exact calculations or using the diagrams in appendix A.

can be a good approximation for large enough E_T to neglect the tree and disconnected terms all together and set $E_L = E_T$ while performing a local expansion. With this we connect with ref. [1] where the scale E_W is not used to get rid of the non-perturbative contributions. Instead the tree and disconnected terms are neglected, all the entries of $(\Delta H_2)_{rs}$ are approximated by the loop-generated local (up to E_{rs}) operators only and the $\theta(E - E_{rs} - 5m)$ is introduced in eq. (5.51). As explained, neglecting the tree and disconnected terms is justified, while the introduction of $\theta(E - E_{rs} - 5m)$ and truncating the local expansion in practice largely reduce the values of the high energy entries with respect to the exact result. All of these effectively act as our scale E_W. Therefore we see that in many cases our approach and the one in ref. [1] can give similar results.

Even though the numerical results are similar, our approach introduces new tools and insights that we think improve the renormalized Hamiltonian truncation method and can help to develop it further.

6 Conclusion and outlook

In this paper we have developed further the Hamiltonian truncation method. In particular we have explained a way to compute the corrections to the truncated Hamiltonian at any order in the large E_T expansion of $\Delta H = \sum_n \Delta H_n$. We have applied these ideas to scalar field theory in two dimensions and studied the spectrum of the theory as a function of the truncation energy and the coupling constant.

There are various open directions that are very interesting and deserve further investigation. Firstly, it would be a great improvement to the method to find a more precise estimate of the expansion parameter of the series. This estimate should be easy to implement numerically and lead to a precise definition of the cutoff E_W. In this work we have been pragmatic in this respect, and investigated the behaviour of the spectrum as this cutoff is modified. It might be that only removing the contribution of certain type of matrix elements (like the ones corresponding to high occupation number and zero momentum) the series is greatly improved.

We have not pushed the numerical aspects of the method very far and all the computations have been done with `Mathematica`. With more efficient programming languages it would be interesting to further study and check that as the truncation energy E_T is increased the uncertainty in the precise choice of E_W is reduced.

Another point that should be addressed is the dependence of the spectrum on L as higher ΔH_n corrections are added; also it could be relevant to inspect if there are diagrams that dominate for large $Lm \gg 1$.

Another very interesting path to develop further is to apply renormalization group techniques to resum the fixed order calculations of ΔH. Since the exact eigenvalues do not depend on the truncation energy E_T, it may be possible resum the calculation of ΔH_n. Our analytic expressions for the ΔH_n corrections permit a precise study of the possible resummation of the leading corrections at each order in the perturbation theory of the large E_T expansion. One could start by studying the resummation of the leading local

corrections, and for that the phase space formulation that we have introduced is useful as there are simple recursion relations for the differential phase space.

Another fascinating avenue to pursue is the applicability of the method to other theories with higher spin fields and to increase the number of dimensions. In this regard, we notice that the derivation of eqs. (5.22)–(5.24) seems to be formally valid in any space-time dimension d. Recall that the c_i's are the coefficients of the local operators added to H_T to take into account the effect of the highest energetic H_0 eigenstates not included in the light Hilbert space $\mathcal{H}_l$. As d is increased beyond $d = 2$ the UV divergencies appear due to the increasingly rapid growth of the phase space functions $\Phi_i(E)$. One can then regulate the c_i coefficients with a cutoff Λ. For instance, consider the coefficient c_4 of the ϕ^4 operator

$$c_4^\Lambda(\mathcal{E}) = s_2\, g_0^2 \int_{E_L}^\Lambda \frac{dE}{2\pi} \frac{1}{\mathcal{E} - E}\, \Phi_2(E)\,, \tag{6.1}$$

in $d = 4$. Then, requiring that the energy levels are independent of the regulator one finds the following β-function

$$\beta(g) = -\Lambda \frac{\partial c_4^\Lambda}{\partial \Lambda} + \mathcal{O}(g^3) = \frac{s_2 g^2}{2\pi} \Phi_2(\Lambda) + \mathcal{O}(g^3, \mathcal{E})\,, \tag{6.2}$$

where the $\mathcal{E}$ corrections can be neglected in the limit of large $\Lambda \gg \mathcal{E}$. Redefining $g \equiv \lambda/4!$ one recovers the known result for the $\lambda \phi^4$ theory $\beta(\lambda) = \frac{3}{16\pi^2}\lambda^2 + \mathcal{O}(\lambda^3)$, where we have neglected the mass corrections that for $\Lambda \gg m$ decouple as $\Phi_2(\Lambda) = 1/(8\pi) + \mathcal{O}(m^2/\Lambda^2)$. A possible way to make contact between the calculation in the renormalized Hamiltonian method and the standard calculation of the beta function is by noticing that the coefficient of the divergent part of the amplitude is proportional to the coefficient of its finite imaginary part which in turn (by the optical theorem) is proportional to the two-particle phase space. It would be very interesting to further study RG flows from the perspective of the renormalized Hamiltonian truncation method approach.

We think that the Hamiltonian truncation method is a very promising approach to study strong dynamics, and that there are still open important questions to be addressed.

Acknowledgments

A   Diagramatic representation

There is a simple and powerful diagrammatic representation that permits to easily find the expression for ΔH_n. This can be used to either compute the full operator ΔH_n or

the leading $\mathcal{O}(t^0, z^0)$ coefficients in the local expansion of ΔH_{n+} defined in section 4. This representation is valid for any ϕ^α theory, but here we give examples only for the ϕ^4 case for concreteness.

Local coefficients. Imagine that we want to find the local coefficients $\mathcal{O}(t^0, z^0)$ for $\Delta H_{3+}^{\phi^2}$. To find them one puts 3 vertices ordered horizontally[22] and draws all possible diagrams that have only 2 external lines, four lines meeting at each vertex and don't have any lines starting and ending at the same vertex. Next, we assign a momentum for each internal line and draw a vertical line between every pair of vertices. One such diagrams is

(A.1)

The expression corresponding to a given diagram with n vertices and N propagators is given by

$$ sg^n \sum_{k's} \frac{1}{\prod_{i=1}^{N}(2L\omega_{k_i})} \prod_{p=1}^{n-1} L\,\delta_p \frac{\theta\big(\sum_{k_j \in \{s_p\}} \omega_{k_j} - E_L\big)}{\mathcal{E} - \sum_{k_j \in \{s_p\}} \omega_{k_j}}\,, \tag{A.2} $$

where $k_j = 2\pi n_j/L$ with $n_j \in \mathbb{Z}$. Each of the $n-1$ sets of momenta $\{s_p\}$ consist in the momenta of the internal lines that are cut by each vertical line. In (A.1) these would be $s_1 = \{k_1, k_2, k_5\}$ and $s_2 = \{k_3, k_4, k_5\}$. The symbol δ_p stands for a Kronecker delta that imposes that the total momentum crossing a cut is zero; s is a symmetry factor that counts all the ways that the lines of the vertices can be connected to form the diagram. Applying this recipe to the diagram in (A.1) one has

 $= s_4^{221}\, g^3 \sum_{k's} \frac{L^2 \delta_{k_1+k_2+k_5,0}^{k_3+k_4+k_5,0}}{\prod_{i=1}^5 (2L\omega_{k_i})} \frac{\theta(\omega_{k_1}+\omega_{k_2}+\omega_{k_5}-E_L)}{\mathcal{E}-\omega_{k_1}-\omega_{k_2}-\omega_{k_5}} \frac{\theta(\omega_{k_3}+\omega_{k_4}+\omega_{k_5}-E_L)}{\mathcal{E}-\omega_{k_3}-\omega_{k_4}-\omega_{k_5}}\,.$

(A.3)

where the symmetry factor s_p^{mnv} is given in eq. (4.20). Another example of a contribution to $\Delta H_{3+}^{\phi^2}$ would be

 $= s_4^{212}\, g^3 \sum_{k's} \frac{L^2 \delta_{k_3+k_4+k_5,0}^{k_1+k_2+k_3+k_4,0}}{\prod_{i=1}^5 (2L\omega_{k_i})} \frac{\theta(\Sigma_{s=1}^5 \omega_{k_s}-E_L)}{\mathcal{E}-\omega_{k_1}-\omega_{k_2}-\omega_{k_3}-\omega_{k_4}} \frac{\theta(\Sigma_{s=1}^4 \omega_{k_s}-E_L)}{\mathcal{E}-\omega_{k_3}-\omega_{k_4}-\omega_{k_5}}\,.$

(A.4)

Notice that the ordering of the vertices matters since the diagrams of (A.3) and (A.4) have the same topology but give different results.

With this prescription one easily recovers eqs. (5.11), (5.13), and (5.15) corresponding to the ΔH_{2+} coefficients in the ϕ^4 theory

$$ c_0 = \text{}\,, \qquad c_2 = \text{}\,, \qquad c_4 = \text{}\,. \tag{A.5} $$

---

[22]The vertices are ordered in a line because the $V(T_s)$'s in eq. (2.3) are time-ordered in the whole integration domain. This is in contrast with the standard Feynman diagrams in the calculation of an n-point function, where each space-time integral is over the whole real domain.

Notice that to include the contributions E_{rs} mentioned at the end of section 5.2 the same diagrammatic representation applies but one must then substitute $\mathcal{E} \to \mathcal{E} - E_{rs}$ in eq. (A.2) making the coefficients depend on the matrix entry.

Exact ΔH_n opertors. A similar diagrammatic representation can be used to calculate the exact $\Delta \widehat{H}_n$ operator from which one can easily get ΔH_n. The prescription to follow is very similar to the one for the local case, where one starts drawing the same diagrams and putting vertical lines between every pair of vertices. The only difference is that now one extends the external lines to left and right in all possible combinations for each diagram drawn and also assigns a momentum to the external lines. For the diagram in (A.1) this means
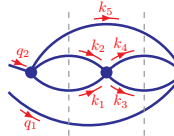

$$
\hspace{10cm} . \tag{A.6}
$$
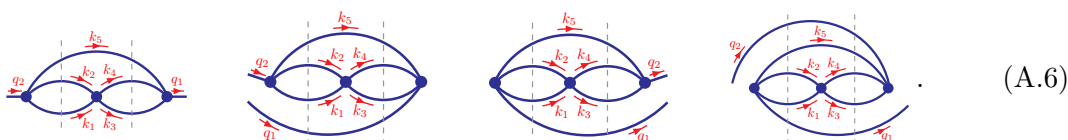
Now, the operator corresponding to a given diagram with n vertices, N propagators, A external lines starting left and B external lines starting right is

$$
\kappa s g^n \sum_{k's,q's} \frac{1}{\prod_{i=1}^N (2L\omega_{k_i})} \prod_{p=1}^{n-1} \frac{\theta\big(\omega_{rs} + \sum_{Q_j \in \{s_p\}} \omega_{Q_j} - E_L\big)}{\mathcal{E} - \omega_{rs} - \sum_{Q_j \in \{s_p\}} \omega_{Q_j}} \prod_{\alpha=1}^n L\delta_\alpha \prod_{r=A+1}^{A+B} \frac{a_{q_r}^\dagger}{\sqrt{2L\omega_{q_r}}} \prod_{l=1}^A \frac{a_{q_l}}{\sqrt{2L\omega_{q_l}}}, \tag{A.7}
$$

where the sums over $k's$, $q's$ sum over all possible momenta for a given k_i, q_i. Then, each of the $n-1$ sets of momenta $\{s_p\}$ consists in the momenta of the lines that are cut by each vertical line. For the first diagram from the left in (A.7) these would be $s_1 = \{k_1, k_2, k_5\}$ and $s_2 = \{k_3, k_4, k_5\}$, and for the second one $s_1 = \{q_1, k_1, k_2, k_5\}$ and $s_2 = \{q_1, k_3, k_4, k_5\}$. The symbol δ_α stands for a Kronecker delta that imposes momentum conservation at each vertex α. The symbol ω_{rs} depends on the energy of the states $\langle E_r |, | E_s \rangle$ on which a and $a^\dagger$ act i.e. it is different for each entry $\left(a_{-q_r}^\dagger a_{q_l}\right)_{rs}$, and is given by $w_{rs} \equiv E_{rs} - \frac{1}{2} \sum_{i=1}^{A+B} \omega_{q_i}$ where $E_{rs} = (E_r + E_s)/2$. As before s is a symmetry factor that counts all the ways that the lines of the vertices can be connected to form the diagram. Lastly κ counts all the equivalent ways that the external lines coming out from the same vertex can be ordered left and right, for the diagrams in (A.7) is is always one, since there is only one external line per vertex. Applying this recipe to the first and second diagrams in (A.7) one has

$$
\begin{aligned}
\text{} &= s_4^{221}\, g^3 \sum_{k_1, \cdots, k_5} \sum_{q_1, q_2} \frac{L^2 \delta_{k_1+k_2+k_5, q_1}^{k_3+k_4+k_5, q_2}}{\prod_{i=1}^5 (2L\omega_{k_i})} \frac{\theta(\omega_{rs} + \omega_{k_1} + \omega_{k_2} + \omega_{k_5} - E_L)}{\mathcal{E} - \omega_{rs} - \omega_{k_1} - \omega_{k_2} - \omega_{k_5}} \\
&\times \frac{\theta(\omega_{rs} + \omega_{k_3} + \omega_{k_4} + \omega_{k_5} - E_L)}{\mathcal{E} - \omega_{rs} - \omega_{k_3} - \omega_{k_4} - \omega_{k_5}} L\delta_{k_3+k_4, k_1+k_2} \frac{a_{q_1}^\dagger a_{q_2}}{2L\sqrt{\omega_{q_1} \omega_{q_2}}},
\end{aligned} \tag{A.8}
$$

$$
\begin{aligned}
\includegraphics{diagram} = s_4^{221}\, g^3 \sum_{k_1,\cdots,k_5}\sum_{q_1,q_2} & \frac{L^2 \delta_{k_1+k_2+k_5+q_1,0}^{k_3+k_4+k_5+q_1,0}}{\prod_{i=1}^{5}(2L\omega_{k_i})}\,\frac{\theta(\omega_{rs}+\omega_{k_1}+\omega_{k_2}+\omega_{k_5}+\omega_{q_1}-E_L)}{\mathcal{E}-\omega_{rs}-\omega_{k_1}-\omega_{k_2}-\omega_{k_5}-\omega_{q_1}} \\
& \times \frac{\theta(\omega_{rs}+\omega_{k_3}+\omega_{k_4}+\omega_{k_5}+\omega_{q_1}-E_L)}{\mathcal{E}-\omega_{rs}-\omega_{k_3}-\omega_{k_4}-\omega_{k_5}-\omega_{q_1}}\,L\delta_{q_1+q_2,0}\frac{a^\dagger_{-q_1}a_{q_2}}{2L\sqrt{\omega_{q_1}\omega_{q_2}}}\,,
\end{aligned}
$$
$$(A.9)$$

where $\omega_{rs}=E_{rs}-(\omega_{q_1}+\omega_{q_2})/2$ and the symmetry factor s_p^{mnv} is given in eq. (4.20).

With this set of rules one can easily get the expression for $\Delta\widehat{H}_2$ and $\Delta\widehat{H}_3$ for the ϕ^2 and ϕ^4 theories. Then one finds ΔH_2 and ΔH_3 by keeping only the contributions with all poles $\mathcal{E}>E_T$.

B $\quad\Delta H$ for the ϕ^2 perturbation

B.1 Two-point correction

In this section we give the full expressions of the $\Delta\widehat{H}_2$ corrections for the scalar theory with potential $V=g_2\int dx\,\phi^2$. Recall that the symmetry factor is given by $s_p=\binom{2}{p}^2 p!$. We will use the prescription $E_{rs}=(E_r+E_s)/2$ where E_r and E_s are H_0 eigenvalues.

$$
\Delta\widehat{H}_2^{\mathbb{1}}(\mathcal{E})_{rs} = g_2^2 s_2 \frac{1}{2^2}\sum_k \frac{1}{\omega_k^2}\frac{1}{\mathcal{E}-E_{rs}-2\omega_k}\delta_{rs}
\tag{B.1}
$$

$$
\begin{aligned}
\Delta\widehat{H}_2^{\phi^2}(\mathcal{E})_{rs} = g_2^2 s_1 \frac{1}{2^2}\sum_q \frac{1}{\omega_q^2}\Bigg[& \left(a_q a_{-q}\frac{1}{\mathcal{E}-E_{rs}-\omega_q} + \text{h.c.}\right) \\
& + a_q^\dagger a_q \left(\frac{1}{\mathcal{E}-E_{rs}-2\omega_q}+\frac{1}{\mathcal{E}-E_{rs}}\right)\Bigg]
\end{aligned}
\tag{B.2}
$$

$$
\begin{aligned}
\Delta\widehat{H}_2^{\phi^4}(\mathcal{E})_{rs} = g_2^2 s_0 \frac{1}{2^2}\sum_{q_1,q_2}\frac{1}{\omega_{q_1}\omega_{q_2}}\Bigg[& a_{q_1}a_{q_2}a_{-q_1}a_{-q_2}\frac{1}{\mathcal{E}-E_{rs}-\omega_{q_1}+\omega_{q_2}} + \text{h.c.} \\
& + 2\,a_{q_1}^\dagger a_{q_1}a_{q_2}a_{-q_2}\left(\frac{1}{\mathcal{E}-E_{rs}+\omega_{q_2}}+\frac{1}{\mathcal{E}-E_{rs}-\omega_{q_2}}\right)+\text{h.c.} \\
& + a_{q_1}^\dagger a_{-q_1}^\dagger a_{q_2}a_{-q_2}\left(\frac{1}{\mathcal{E}-E_{rs}+\omega_{q_1}+\omega_{q_2}}+\frac{1}{\mathcal{E}-E_{rs}-\omega_{q_1}-\omega_{q_2}}\right) \\
& + 4\,a_{q_1}^\dagger a_{q_2}^\dagger a_{q_1}a_{q_2}\frac{1}{\mathcal{E}-E_{rs}}\Bigg]\,.
\end{aligned}
\tag{B.3}
$$

B.2 Three-point correction

In this section we give the full expressions of the ΔH_3 corrections for the scalar theory with potential $V=g_2\int dx\,\phi^2$. Recall that the symmetry factor is given by

$$
s_p^{mnv} = \frac{p!^3}{(p-m-n)!(p-m-v)!(p-n-v)!\,m!\,n!\,v!}\,.
\tag{B.4}
$$

We use the notation $\Delta H_3 = \Delta H_3^{\mathbb{1}} + \Delta H_3^{\phi^2} + \Delta H_3^{\phi^4} + \Delta H_3^{\phi^6}$, where

$$\Delta H_3^{\mathbb{1}}(\mathcal{E})_{rs} = \frac{g_2^3 s_2^{111}}{2^3} \sum_k \frac{1}{\omega_{k_1}\omega_{k_2}\omega_{k_3}} G_0(k_1, k_2, k_3, E_T)\,, \tag{B.5}$$

$$\Delta H_3^{\phi^2}(\mathcal{E})_{rs} = \frac{g_2^3}{2^3} \sum_{k,q} \frac{1}{\omega_{k_1}\omega_{k_2}} \frac{1}{\sqrt{\omega_{q_1}\omega_{q_2}}} \big[s_2^{200} G_{2,1}(k_1, k_2, q_1, q_2, E_T)$$
$$+ s_2^{110} G_{2,2}(k_1, k_2, q_1, q_2, E_T) \big]\,, \tag{B.6}$$

$$\Delta H_3^{\phi^4}(\mathcal{E})_{rs} = \frac{g_2^3 s_2^{100}}{2^3} \sum_{k,q} \frac{1}{\omega_k} \frac{1}{\sqrt{\omega_{q_1}\cdots\omega_{q_4}}} G_4(k, q_1, \ldots, q_4)\,, \tag{B.7}$$

$$\Delta H_3^{\phi^6}(\mathcal{E})_{rs} = \frac{g_2^3 s_2^{000}}{2^3} \sum_q \frac{1}{\sqrt{\omega_{q_1}\cdots\omega_{q_6}}} G_6(q_1, \ldots, q_6)\,, \tag{B.8}$$

where

$$G_0 = \delta_{k_1+k_2,0}\delta_{k_1+k_3,0}\, [f_0]^{12}[f_0]^{13}\,, \tag{B.9}$$

$$G_{2,1} = a_{q_1} a_{q_2}\, \delta_0 \delta_{k_1+k_2,0}\, [f_2]_{12}^{12}[f_2]^{12} + \text{h.c.} + 2 a_{q_1}^\dagger a_{q_2}\, \delta_1 \delta_{k_1+k_2,0}\, [f_2]_1^{12}[f_2]_2^{12}\,, \tag{B.10}$$

$$G_{2,2} = a_{q_1}^\dagger a_{q_2}\, \delta_1 \delta_{k_1+q_1,0}\delta_{k_1+k_2,0}\big([f_2]_{12}^1[f_2]_1^{12} + [f_2]_{12}^1[f_2]_2^{12} + [f_2]_{12}^1[f_2]_{12}^2\big)\,, \tag{B.11}$$

$$\begin{aligned} G_4 = &\, a_{q_1}^\dagger a_{q_2} a_{q_3} a_{q_4}\, \delta_1 \delta_{k+q_1,0}\delta_{q_3+q_4,0}[f_4]_{1234}^1[f_4]_{12}^1 + \text{h.c.} \\ &+ 2 a_{q_1}^\dagger a_{q_2}^\dagger a_{q_3} a_{q_4}\, \delta_2 \delta_{q_1-q_3,0}\delta_{k+q_2,0}[f_4]_{124}^1[f_4]_{234}^1 \\ &+ a_{q_1}^\dagger a_{q_2}^\dagger a_{q_3} a_{q_4}\, \delta_2 \big(\delta_{q_1+q_2,0}\delta_{k+q_4,0}[f_4]_{1234}[f_4]_{124}^1 + \delta_{q_3+q_4,0}\delta_{k+q_1,0}[f_4]_{1234}[f_4]_{124}^1\big)\,, \end{aligned} \tag{B.12}$$

$$\begin{aligned} G_6 = &\, a_{q_1}^\dagger a_{q_2}^\dagger a_{q_3} a_{q_4} a_{q_5} a_{q_6}\, \delta_2 \delta_{q_1+q_2,0}\delta_{q_3+q_4,0}[f_6]_{123456}[f_6]_{1234} + \text{h.c.} \\ &+ 2 a_{q_1}^\dagger a_{q_2}^\dagger a_{q_3}^\dagger a_{q_4} a_{q_5} a_{q_6}\, \delta_3 \delta_{q_1+q_2,0}\delta_{q_5+q_6,0}[f_6]_{12356}[f_6]_{12456}\,. \end{aligned} \tag{B.13}$$

We have defined $w_{rs}^p \equiv E_{rs} - \frac{1}{2}\sum_{i=1}^p \omega_{q_i}$, $\delta_d \equiv \delta_{\Sigma_{i=1}^d q_i, \Sigma_{j=d+1}^p q_j}$ (the Kronecker delta that imposes momentum conservation to the creation/annihilation operators) and

$$[f_p]_Q^K = \frac{\theta(\omega_{rs}^p + \Sigma_{i\in\{Q\}}\omega_{q_i} + \Sigma_{i\in\{K\}}\omega_{k_i} - E_T)}{\mathcal{E} - \omega_{rs}^p - \sum_{i\in\{Q\}}\omega_{q_i} - \sum_{i\in\{K\}}\omega_{k_i}}\,. \tag{B.14}$$

C $\quad \Delta H$ for the ϕ^4 theory

In this appendix we give the exact two-point correction and the first terms in the local expansion of the three-point correction. Getting the exact three-point correction would be straightforward.

C.1 Two-point correction

In this appendix we give the full expressions of the ΔH_2 for the ϕ^4 theory. Using the notation $\Delta H_2 = \sum_{n=0}^{8} \Delta H_2^{\phi^n}$ we have

$$\Delta H_2^{\mathbb{1}}(\mathcal{E}, E_T) = \frac{s_4 g^2}{2^4 L^2} \sum_{k_1 k_2 k_3 k_4} \frac{1}{\omega_{k_1} \omega_{k_2} \omega_{k_3} \omega_{k_4}} F_0(k_1, k_2, k_3, k_4, E_T)\,, \tag{C.1}$$

$$\Delta H_2^{\phi^2}(\mathcal{E}, E_T) = \frac{s_3 g^2}{2^4 L^2} \sum_{k_1, k_2, k_3} \sum_{q_1, q_2} \frac{1}{\omega_{k_1} \omega_{k_2} \omega_{k_3}} \frac{1}{\sqrt{\omega_{q_1} \omega_{q_2}}} F_2(k_1, k_2, k_3, q_1, q_2, E_T)\,, \tag{C.2}$$

$$\Delta H_2^{\phi^4}(\mathcal{E}, E_T) = \frac{s_2 g^2}{2^4 L^2} \sum_{k_1, k_2} \sum_{q_1, q_2, q_3, q_4} \frac{1}{\omega_{k_1} \omega_{k_2}} \frac{1}{\sqrt{\omega_{q_1} \cdots \omega_{q_4}}} F_4(k_1, k_2, q_1, \ldots, q_4, E_T)\,, \tag{C.3}$$

$$\Delta H_2^{\phi^6}(\mathcal{E}, E_T) = \frac{s_1 g^2}{2^4 L^2} \sum_{k} \sum_{q_1, \ldots, q_6} \frac{1}{\omega_k} \frac{1}{\sqrt{\omega_{q_1} \cdots \omega_{q_6}}} F_6(k, q_1, q_2, \ldots, q_6, E_T)\,, \tag{C.4}$$

$$\Delta H_2^{\phi^8}(\mathcal{E}, E_T) = \frac{s_0 g^2}{2^4 L^2} \sum_{q_1, \ldots, q_8} \frac{1}{\sqrt{\omega_{q_1} \cdots \omega_{q_8}}} F_8(q_1, q_2, \ldots, q_8, E_T) \tag{C.5}$$

The F_i functions are given by

$$F_0 = \delta_{k_1 + k_2 + k_3 + k_4, 0} \, [f_0]^{1234} \tag{C.6}$$

$$F_2 = a_{q_1}^\dagger a_{q_2} \delta_1 \delta_{k_1 + k_2 + k_3, q_1} \big([f_2]^{123} + [f_2]_{12}^{123} \big) + a_{q_1} a_{q_2} \delta_0 \delta_{k_1 + k_2 + k_3, q_1} [f_2]_2^{123} + \text{h.c.} \tag{C.7}$$

$$\begin{aligned}
F_4 = &\; a_{q_1} a_{q_2} a_{q_3} a_{q_4} \delta_0 \delta_{k_1 + k_2, q_1 + q_2} [f_4]_{34}^{12} + \text{h.c.} \\
&+ 2 a_{q_1}^\dagger a_{q_2} a_{q_3} a_{q_4} \delta_1 \big(\delta_{k_1 + k_2, q_1 - q_2} [f_4]_2^{12} + \delta_{k_1 + k_2, -q_1 + q_2} [f_4]_{134}^{12} \big) + \text{h.c.} \\
&+ a_{q_1}^\dagger a_{q_2}^\dagger a_{q_3} a_{q_4} \delta_2 \big(\delta_{k_1 + k_2, q_1 + q_2} [f_4]^{12} + \delta_{k_1 + k_2, -q_1 - q_2} [f_4]_{1234}^{12} + 4 \delta_{k_1 + k_2, q_1 - q_3} [f_4]_{14}^{12} \big)
\end{aligned} \tag{C.8}$$

$$\begin{aligned}
F_6 = &\; a_{q_1}^\dagger a_{q_2} a_{q_3} a_{q_4} a_{q_5} a_{q_6} \delta_1 \delta_{k, q_2 + q_3 - q_1} \, 3 \, [f_6]_{1456}^1 + \text{h.c.} \\
&+ a_{q_1}^\dagger a_{q_2}^\dagger a_{q_3} a_{q_4} a_{q_5} a_{q_6} \delta_2 \big(9 \, \delta_{k, q_3 + q_4 - q_1} [f_6]_{156}^1 + 3 \, \delta_{k, q_3 - q_1 - q_2} [f_6]_{12456}^1 \big) + \text{h.c.} \\
&+ a_{q_1}^\dagger a_{q_2}^\dagger a_{q_3}^\dagger a_{q_4} a_{q_5} a_{q_6} \delta_3 \big(9 \, \delta_{k, q_4 + q_5 - q_1} [f_6]_{16}^1 + 9 \delta_{k, -q_4 - q_5 + q_1} [f_6]_{2345}^1 + \delta_{k + q_1 + q_2 + q_3, 0} [f_6]_{123456}^1 \big)
\end{aligned} \tag{C.9}$$

$$\begin{aligned}
F_8 = &\; a_{q_1}^\dagger a_{q_2}^\dagger a_{q_3} a_{q_4} a_{q_5} a_{q_6} a_{q_7} a_{q_8} \delta_2 \, 6 \delta_{q_1 + q_2 - q_3 - q_4, 0} [f_8]_{125678} + \text{h.c.} \\
&+ a_{q_1}^\dagger a_{q_2}^\dagger a_{q_3}^\dagger a_{q_4} a_{q_5} a_{q_6} a_{q_7} a_{q_8} \delta_3 \big(24 \delta_{q_1 + q_2 - q_4 - q_5} [f_8]_{12678} + 4 \delta_{q_1 + q_2 + q_3 - q_4} [f_8]_{1235678} \big) + \text{h.c.} \\
&+ a_{q_1}^\dagger a_{q_2}^\dagger a_{q_3}^\dagger a_{q_4}^\dagger a_{q_5} a_{q_6} a_{q_7} a_{q_8} \delta_4 \Big(16 \delta_{q_1 - q_5 - q_6 - q_7, 0} \big([f_8]_{18} + [f_8]_{234567} \big) \\
&\qquad\qquad + 36 \delta_{q_1 + q_2 - q_5 - q_6, 0} [f_8]_{1278} + \delta_{q_1 + q_2 + q_3 + q_4, 0} [f_8]_{12345678} \Big)\,.
\end{aligned} \tag{C.10}$$

We have defined $w_{rs}^p \equiv E_{rs} - \frac{1}{2} \sum_{i=1}^{p} \omega_{q_i}$, $\delta_d \equiv \delta_{\Sigma_{i=1}^d q_i, \Sigma_{j=d+1}^p q_j}$ (the Kronecker delta that imposes momentum conservation to the creation/annihilation operators) and

$$[f_p]_Q^K = \frac{\theta(\omega_{rs}^p + \Sigma_{i \in \{Q\}} \omega_{q_i} + \Sigma_{i \in \{K\}} \omega_{k_i} - E_T)}{\mathcal{E} - \omega_{rs}^p - \sum_{i \in \{Q\}} \omega_{q_i} - \sum_{i \in \{K\}} \omega_{k_i}}\,. \tag{C.11}$$

References

[1] S. Rychkov and L.G. Vitale, *Hamiltonian truncation study of the ϕ^4 theory in two dimensions*, *Phys. Rev.* **D 91** (2015) 085011 [arXiv:1412.3460] [INSPIRE].

[2] S. Rychkov and L.G. Vitale, *Hamiltonian truncation study of the ϕ^4 theory in two dimensions. II. The $\mathbb{Z}_2$ -broken phase and the Chang duality*, *Phys. Rev.* **D 93** (2016) 065014 [arXiv:1512.00493] [INSPIRE].

[3] M. Hogervorst, S. Rychkov and B.C. van Rees, *Truncated conformal space approach in d dimensions: a cheap alternative to lattice field theory?*, *Phys. Rev.* **D 91** (2015) 025005 [arXiv:1409.1581] [INSPIRE].

[4] V.P. Yurov and A.B. Zamolodchikov, *Truncated conformal space approach to scaling Lee-Yang model*, *Int. J. Mod. Phys.* **A 5** (1990) 3221 [INSPIRE].

[5] S.J. Brodsky, H.-C. Pauli and S.S. Pinsky, *Quantum chromodynamics and other field theories on the light cone*, *Phys. Rept.* **301** (1998) 299 [hep-ph/9705477] [INSPIRE].

[6] D. Lee, N. Salwen and D. Lee, *The diagonalization of quantum field Hamiltonians*, *Phys. Lett.* **B 503** (2001) 223 [hep-th/0002251] [INSPIRE].

[7] D. Lee, N. Salwen and M. Windoloski, *Introduction to stochastic error correction methods*, *Phys. Lett.* **B 502** (2001) 329 [hep-lat/0010039] [INSPIRE].

[8] N. Salwen, *Non-perturbative methods in modal field theory*, Ph.D. Thesis, Harvard University (2001) [hep-lat/0212035] [INSPIRE].

[9] M. Windoloski, *A non-perturbative study of three-dimensional quartic scalar field theory using modal field theory*, Ph.D. Thesis, University of Massachusetts Amherst (2000).

[10] E.D. Brooks III and S.C. Frautschi, *Scalars coupled to fermions in (1+1)-dimensions*, *Z. Phys.* **C 23** (1984) 263 [INSPIRE].

[11] E. Katz, G. Marques Tavares and Y. Xu, *Solving 2D QCD with an adjoint fermion analytically*, *JHEP* **05** (2014) 143 [arXiv:1308.4980] [INSPIRE].

[12] E. Katz, G. Marques Tavares and Y. Xu, *A solution of 2D QCD at finite N using a conformal basis*, arXiv:1405.6727 [INSPIRE].

[13] S.S. Chabysheva and J.R. Hiller, *Basis of symmetric polynomials for many-boson light-front wave functions*, *Phys. Rev.* **E 90** (2014) 063310 [arXiv:1409.6333] [INSPIRE].

[14] P. Giokas and G. Watts, *The renormalisation group for the truncated conformal space approach on the cylinder*, arXiv:1106.2448 [INSPIRE].

[15] M. Lencsés and G. Takács, *Excited state TBA and renormalized TCSA in the scaling Potts model*, *JHEP* **09** (2014) 052 [arXiv:1405.3157] [INSPIRE].

[16] A. Coser, M. Beria, G.P. Brandino, R.M. Konik and G. Mussardo, *Truncated conformal space approach for 2D Landau-Ginzburg theories*, *J. Stat. Mech.* (2014) P12010 [arXiv:1409.1494] [INSPIRE].

[17] M. Lencses and G. Takács, *Confinement in the q-state Potts model: an RG-TCSA study*, *JHEP* **09** (2015) 146 [arXiv:1506.06477] [INSPIRE].

[18] M. Lüscher, *Volume dependence of the energy spectrum in massive quantum field theories. I. Stable particle states*, *Commun. Math. Phys.* **104** (1986) 177 [INSPIRE].

[19] M. Lüscher, *Volume dependence of the energy spectrum in massive quantum field theories. II. Scattering states*, *Commun. Math. Phys.* **105** (1986) 153 [INSPIRE].